| Haplotype | ART3-SNP# | | | | | Freq (EM) | | $\chi^2$ | P-value |
|---|---|---|---|---|---|---|---|---|---|
| | 1 | 5 | 23 | 25 | 28 | Control | NOA | | |
| H1 | C | C | A | G | C | 35.3% | 26.6% | 15.7 | 0.000073 |
| H2 | T | T | G | A | T | 27.5% | 28.5% | 0.21 | 0.65 |
| H3 | T | T | A | G | T | 13.8% | 13.4% | 0.04 | 0.84 |
| H4 | T | C | A | G | T | 7.2% | 6.4% | 0.47 | 0.50 |
| H5 | C | T | A | A | C | 3.0% | 4.6% | 3.10 | 0.078 |
| H6 | T | C | A | G | C | 2.6% | 3.2% | 0.42 | 0.52 |
| H7 | T | C | G | G | T | 1.7% | 3.0% | 3.22 | 0.07 |
| H8 | C | T | A | G | T | 2.0% | 1.7% | 0.16 | 0.69 |
| H9 | T | T | A | A | C | 1.2% | 1.7% | 0.87 | 0.35 |
| H10 | T | T | A | G | C | 1.5% | 1.0% | 0.62 | 0.43 |
| Others | | | | | | 4.2% | 9.9% | | |

**Figure 6.** Haplotype-based Association Study of *ART3*

The expectation-maximization (EM) algorithm [37] was used to infer *ART3* haplotype frequencies with genotyping data of five tag SNPs, ART3-SNP1, 5, 8, 23, 25, and 28 (see Table 4). At the respective SNP sites, red and blue boxes represent minor and major alleles, respectively.
doi:10.1371/journal.pgen.0040026.g006

protein expression among the three *ART3* diplo-groups carrying none, one, or two copies of haplotype H1.

## Discussion

### Genomic Analysis of NOA

Our investigation was designed to clarify the pathogenesis of NOA using global gene expression analyses of testis samples from NOA patients and to identify genetic susceptibilities underlying NOA from the genes differentially expressed. Large families with multiple generations having NOA cannot be expected due to the nature of infertility, so linkage study is impractical for NOA and has not been reported. Alternatively, allelic association study is a practical approach to identification of genetic susceptibility underlying NOA. Thus far, more than 80 genes have been identified as essential for male infertility in humans and mice [3]. Genes on the Y chromosome were emphasized because of observed microdeletions in patients, and genes such as DAZ and HSFY were examined for possible susceptibility genes [28,29]. Recently, homozygous mutation of the aurora kinase C gene was identified in large-headed multiflagellar polyploid spermatozoa, a rare form of infertility, using homozygosity mapping [30]. In the current study, we applied a novel approach to identify common susceptibility genes for NOA by applying global gene expression analysis of NOA testes. Based on the hypothesis that a common variant of a susceptibility gene has resulted in altered expression in tissues relevant to disease etiology [31], we first elucidated the gene expression profile in testes of NOA patients and characterized the genetic pathways that were either underexpressed or over-expressed. Because spermatogenesis is a complex differentiation process, NOA could result from a defect at any stage of the process. Thus, gene expression profiling of NOA tissues might well be confounded by the difficulty of discerning the differential stage and the pathological status. Feig et al. [4] examined stage-specific gene expression profiles in human NOA patients after classification on the basis of Johnsen's score. The testis tissues were classified into four groups showing Sertoli-cell only syndrome, meiotic arrest, testicular hypospermia, and testic-
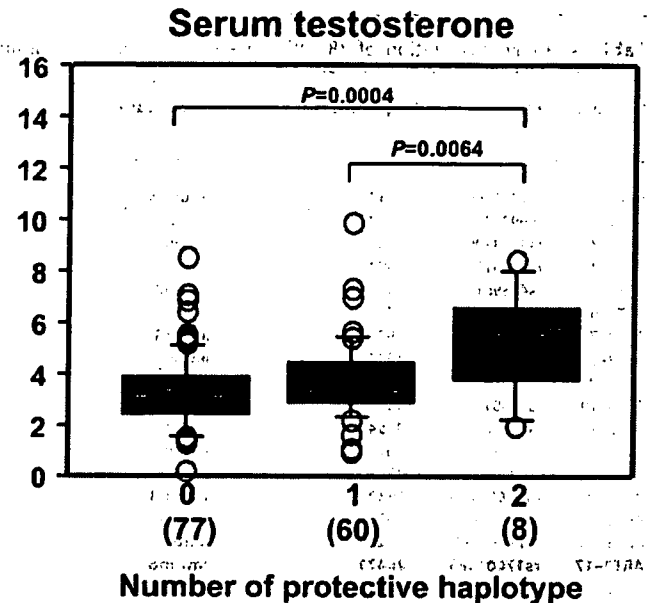


## Serum testosterone

**Figure 7.** Diplotype-Specific Differences in Serum Testosterone Levels in NOA Patients

Three diplo-groups (code 0, 1, and 2) were defined by the number of *ART3* haplotype H1 carried. The serum testosterone levels were significantly different among the three groups (Kruskal-Wallis; df = 2, p = 0.0093) by Bonferroni/Dunn post hoc test.
doi:10.1371/journal.pgen.0040026.g007

ular normospermia, corresponding to Johnsen's score 2, 5, 8, and 10, respectively, and stage-specific differential gene expression was monitored. We sought to identify susceptibility genes underlying NOA that could affect any stage of spermatogenesis. Testis samples subgrouped according to Johnsen's score in advance might identify genes affecting multiple stages of spermatogenesis. Therefore, we globally subgrouped the samples at diverse stages of differentiation using an NMF method for reducing multidimensionality that is appropriate for application to high dimensional biological data. The NMF method subgrouped three classes; NOA1, NOA2, and NOA3, which also were unequivocally subgrouped by the HC approach (Figure 3). Notably, NOA1 and NOA2 represent a pathologically similar type showing low Johnsen's score, but were subclassified because of their distinct gene expression pattern. NOA1 and NOA2 showed differences in LH, FSH, and testosterone levels, thus establishing meaningful biological significance of the sub-classes (Table 2).

### Genetic Susceptibility to NOA

In the current study, we adopted a novel approach to select candidate susceptibility genes for NOA. Global gene expression analyses were performed on NOA testes, and 52 genes were selected according to differential gene expression between NOA subclasses with a strict statistical criterion ($p$ < 0.01 with Tukey's post hoc test). Despite the fact that our selection criteria relied only on data regarding differences in gene expression and did not include any biological assumptions, many of the genes were related to spermatogenesis based on Gene Ontology analyses (Figure 4; Table 1). 191 SNPs of 42 genes were screened, and only one gene, *ART3*, showed a positive association after the two rounds of screening. Multiple SNPs of *ART3* were significantly associ-
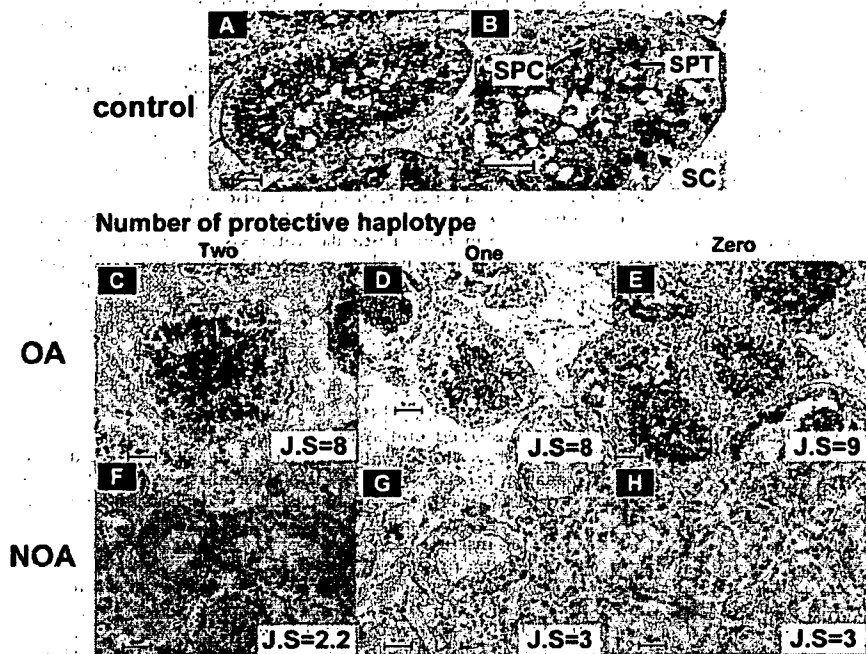
**Figure 8.** Immunohistochemical Analysis of ART3 Expression in Human Testes
Representative seminiferous tubules in testicular sections from normal controls (A, B), OA (C–E), and NOA patients (F–H) are shown. Arrows indicate spermatocytes (SPC); spermatids (SPT); and Sertoli cells (SC) (B). ART3 protein was immunostained with anti-ART3 antibody; ART3-positive spermatocytes (SPC) are noted as brown staining cells (A–E). No marked differences in testicular ART3 expression among the three ART3 diplo-groups carrying none, one, or two copies of the protective haplotype H1were observed in OA (C–E) and NOA (F–H) patients. Magnification is 60× except in (B) (120×).
doi:10.1371/journal.pgen.0040026.g008

ated with NOA, the most significant association being observed with ART3-SNP25 (rs6836703, nominal $p = 0.0025$, permutation $p = 0.034$; Table 4). We also detected a protective haplotype, H1, which was the most common form and was strongly associated with NOA (nominal $p = 0.000073$, corrected $p = 0.00080$, Figure 6). In addition, diplotype analysis showed that individuals carrying at least one haplotype H1 showed an elevated plasma testosterone level (Figure 7).

## Functional Relevance of ART3 in the Pathogenesis of NOA

ART3 is a member of the mono-ADP-ribosyltransferase family genes. The biological function of ART3 remains obscure, as ART3 does not display any detectable arginine-specific transferase activity due to lack of the active site motif (R-S-EXE) that is essential for catalytic activity. Since differentiation of stage-specific expression of ART3 in testis has been reported, protein expression being exclusively present in spermatocytes but absent in spermatozoa [32], a genetic variation of ART3 might well lead to a functional defect in the process of spermatogenesis. Haplotype H1 of ART3, comprising all of the disease-protective alleles at the respective SNP sites, was under-represented in the patients. However, functional disturbance associated with haplotype H1 is so far undetermined despite the fact that several experiments designed to demonstrate haplotype-specific differences in expression level have been performed. Thus, it is possible that this haplotype represents fine tuning that maintains normal maturation of spermatocytes and improves the efficiency of spermatogenesis.

In conclusion, genome-wide gene expression analyses

identified differentially expressed genes of NOA subclasses, and ART3 was identified as a susceptibility gene underlying NOA. This genetic study constitutes only first-stage evidence of association because only Japanese individuals were included, so further replication in independent case-control samples is required to confirm the role of the ART3 haplotype in genetic risk for NOA. Although further functional evidence is also required, these results provide insight into the pathoetiology of NOA as well as reproductive fitness at the molecular level, and suggest a target for therapy.

## Materials and Methods

**Participants.** Testicular biopsy specimens for microarray analysis were obtained from 47 Japanese patients (aged from 24 to 52 years) with NOA and 11 (aged from 22 to 57 years) with OA, each of whom also underwent testicular sperm extraction (TESE) for assisted reproduction and/or diagnostic biopsy for histological examination. The biopsies for microarray analysis and histological examination were mainly sampled from unilateral, multiple testicular sites in the respective patients. Each patient was first assigned to azoospermia by showing no ejaculated spermatozoa in a semen examination. Subsequently, OA was defined as follows: (1) motile spermatozoa were sampled from microsurgical epididymal sperm aspiration (MESA), or (2) a considerable number of mature spermatozoa was sampled from TESE. NOA was tentatively defined as having no epididymal and/or testicular spermatozoa. The degree of spermatogenic defect was histologically evaluated according to Johnsen's score [11]. At least three biopsies from the same individual were taken, and the average Johnsen's scores in the NOA and OA groups ranged from 1 to 6.5 and from 5.1 to 9, respectively. In most patients, preoperative levels of serum follicle-stimulating hormone (FSH), leutenizing hormone (LH), and total testosterone were measured. The infertile male patients who visited Niigata University, Tachikawa Hospital, and St. Mother's Hospital received a routine semen examination according to 1999 WHO criteria. Based on this analysis, sperm were counted

and the patients who had no ejaculated sperms were enrolled for a case-control association study. In total, 442 patients were ascertained to have NOA. In the current study, azoospermia patients with varicocele, ejaculatory dysfunction, endocrinopathy, or histologically examined OA as defined above were excluded. 475 fertile men having no specific clinical record were recruited in Niigata University. The ethics committees of Niigata University, Tachikawa Hospital, St. Mother's Hospital, and Tokai University approved the study protocols, and each participant gave written informed consent. Genomic DNA was prepared from blood white cells by Dneasy (Qiagen, Tokyo, Japan) or salivas by phenol/chloroform extraction.

To examine microdeletion of the Y chromosome in a subset of NOA patients, PCR-based diagnostic technique was used as follows: PCR amplifications with fluorescence (FAM or HEX)-labeled primers were performed to obtain fragments encompassing each of 13 STS markers in and around azoospermia factor (AZF) regions of the Y chromosome (in AZFa: SY83, SY95 and SY105; in AZFb: SY118, G65320, SY126 and SY136; in AZFc: SY148, SY149, SY152, SY283 and SY1291; in the heterochromatin distal to AZFc: SY166). Primer sequences and PCR conditions are available from the authors on request. PCR-amplified fragments were run on the ABI PRISM 3100 Genetic Analyzer (Applied Biosystems, Tokyo, Japan), and Y-chromosome microdeletion was determined with GENESCAN software (Applied Biosystems).

**Microarray analysis of testis samples.** Total RNA from testicular biopsy was extracted using TRIzol reagent (Invitrogen, Carlsbad, CA, USA) and quantity and quality of the extracted RNA were examined with 2100 Bioanalyzer (Agilent Technologies, Palo Alto, CA, USA) using RNA 6000 Nano LabChip (Agilent Technologies). Human Testis Total RNA (BD Biosciences, San Jose, CA, USA), a histologically normal testicular RNA pooled from 39 Caucasians, was used as a common reference in two-color microarray experiments.

For fluorescent cRNA synthesis, high-quality total RNA (150 ng) was labeled with the Low RNA Input Fluorescent Linear Amplification Kit (Agilent Technologies) according to the manufacturer's instructions. In this procedure, cyanine 5-CTP (Cy5) and cyanine 3-CTP (Cy3) (PerkinElmer, Boston, MA, USA) were used to generate labeled cRNA from the extracted patient RNA and the reference RNA, respectively. Labeled cRNAs (0.75 μg each) from one patient and the common reference were combined and fragmented in a hybridization mixture with the *In Situ* Hybridization Kit Plus (Agilent Technologies). The mixture was hybridized for 17 hours at 65°C to the Agilent Human 1A(v2) Oligo Microarray, which carries 60-mer probes to 18,716 human transcripts. After hybridization, the microarray was washed with SSC buffer, and then scanned in Cy3 and Cy5 channels with the Agilent DNA Microarray Scanner model G2565AA (Agilent Technologies). Signal intensity per spot was generated from the scanned image with Feature Extraction Software ver7.5 (Agilent Technologies) in default setting. Spots that did not pass quality control procedures were flagged and removed for further analysis.

The Lowess (locally weighted linear regression curve fit) method was applied to normalize the ratio (Cy5/Cy3) of the signal intensities generated in each microarray with GeneSpring GX 7.3 (Agilent Technologies). Compared with the expression level of reference RNA, the NOA group, with expression undergoing a 2-fold mean change or more was extracted; the OA group comprised transcripts showing less than 2-fold mean expression change (Figure 1A). Of the transcripts included in both groups, only those with a statistically significant difference in expression between NOA and OA testes (based on lowess-normalized natural log[Cy5/Cy3], Bonferroni's corrected $p <$ 0.05) were counted as NOA-related target genes. To elucidate the molecular subtypes of NOA, we adopted the non-negative matrix factorization (NMF) algorithm, which has been recently introduced to analysis of gene expression data [5,6]. For this analysis, a complete dataset without missing values was generated from raw values of Cy5 intensities for the NOA-related target genes in the NOA samples, and used to clarify NOA heterogeneity using three M-files (available from the following URL; http://www.broad.mit.edu/cgi-bin/cancer/publications/pub_paper.cgi?mode=view&paper_id=89) for MAT-LAB (Mathworks, Natick, MA, USA). According to the subclassification of NOA samples, transcripts differentially expressed between NOA subclasses were determined by one-way ANOVA, followed by Tukey's *post hoc* test in GeneSpring GX. For multiple test corrections in this statistical analysis, we used the Benjamini-Hochberg procedure [33] of controlling the false discovery rate (FDR) at the level of 0.05 or 0.01. To analyze which categories of Gene Ontology were statistically overrepresented among the gene lists obtained, we used GO Browser, an optional tool in GeneSpring GX, where the statistical significance was determined by Fisher's exact test. The microarray data reported in this paper have been deposited in the Gene

Expression Omnibus (GEO, http://www.ncbi.nlm.nih.gov/geo/) database, and are accessible through GEO Series accession number GSE9210.

**Quantitative real-time RT-PCR analysis for validation of between-subclass differences in gene expression.** Quantitative real-time RT-PCR analysis was used to verify the microarray data on 53 transcripts representing differential expressions between NOA subclasses with high significance ($p < 0.01$). Among 53 transcripts, VCX (NM_013452), VCX2 (NM_016378), and VCX3A (NM_016379) were examined as a single transcript because sequence homologies between the three transcripts prevented development of appropriate assays for discrimination. Testicular total RNA (1 μg) subjected to microarray analysis was used as a template in first-strand cDNA synthesis with SuperScript III First-Strand Synthesis System (Invitrogen). Each single-stranded cDNA was diluted one-tenth for a subsequent real-time RT-PCR using SYBR *Premix Ex Taq* (Perfect Real Time) (TAKARA BIO, Otsu, Japan) on the ABI PRISM 7900HT Sequence Detection System (Applied Biosystems) according to the manufacturer's instructions. The PCR primers for 43 transcripts showing between-subclass differences with high significance and *GAPDH* were designed and synthesized by TAKARA BIO Inc., or QIAGEN GmbH (as the QuantiTect Primer Assay). In the real-time RT-PCR analysis for the nine remaining transcripts, we used TaqMan Gene Expression Assays (Applied Biosystems) with TaqMan Universal PCR Master Mix (No AmpErase UNG version) according to the manufacturer's instructions (Applied Biosystems). The detailed information on the primer sequences used and/or the assay system selected are summarized in Table S3. A relative quantification method [34] was used to measure the amounts of the respective genes in NOA testes, normalized to *GAPDH* as an endogenous control, and relative to Human Testis Total RNA (BD Biosciences) as a reference RNA. Statistical significance between NOA subclasses was determined by Kruskal-Wallis test, followed by multiple comparisons; $p < 0.05$ was considered significant.

**SNP selection of candidate genes for NOA and genotyping.** Based on gene expression data of NOA testes, we selected 52 genes (encoding 53 transcripts) as candidates for genetic susceptibilities underlying NOA. SNPs of the candidate genes with minor allele frequency (MAF) > 0.05 were obtained from the NCBI dbSNP database (http://www.ncbi.nlm.nih.gov/SNP/), and applied to an initial screening. Of the 52 candidate genes, 10 genes (CTAG1B, LOC158812, LOC255313, MAGEA2, PEPP-2, TSPY1, TSPY2, VCX3A, VCY, and XAGE1) were excluded from the initial screening because gene-based SNPs with MAF > 0.05 were not found in the public SNP database. A total of 191 SNPs of 42 genes were genotyped in the screening with TaqMan SNP Genotyping Assays on the ABI PRISM 7900HT Sequence Detection System (Applied Biosystems). 190 NOA patients (cases) and 190 fertile men (controls) were genotyped in the first round screening. For genes with at least one SNP showing a discrepancy in MAF of 5% or greater between cases and controls, the sample size was increased to 380 cases and 380 controls in the second round.

After two rounds of initial screening, additional SNPs of *ART3* were selected from dbSNP or identified by direct sequencing of all 12 exons of the gene (Ensemble transcript ID ENST00000355810) and splice acceptor and donor sites in the intron using the genomic DNAs from 95 infertile patients as PCR templates. A total of 38 SNPs of *ART3* were finally genotyped on 442 cases and 475 controls by TaqMan SNP Genotyping Assays or by direct sequencing with BigDye Terminators v3.1 Cycle Sequencing Kit (Applied Biosystems) on ABI PRISM 3700 DNA analyzer.

**Statistical analyses in association study.** Pairwise linkage disequilibrium (LD), using the standard definition of $D'$ and $r^2$ [35,36], was measured with SNPAlyze v5.0 software (DYNACOM, Mobara, Japan). To construct *ART3* haplotypes in phase-unknown samples, tag SNPs of *ART3* were selected with Tagger software [25], incorporated in the Haploview. The expectation-maximization (EM) algorithm [37] and PHASE version 2.1.1 [26,27] was used to infer haplotype frequencies and individual diplotypes for *ART3*. Differences in allelic and haplotype frequencies were evaluated using a case-control design with the chi-square test. For an adjustment of multiple testing, we applied a permutation method with Haploview version 3.32 software, or Bonferroni's method to determine corrected *p*-values.

To investigate association of the *ART3* diplotype with clinical phenotypes such as serum hormone levels, differences among the three categories (code 0, 1, and 2), defined by the number of the most significant haplotype, were statistically examined by Kruskal-Wallis test, followed by Bonferroni/Dunn *post hoc* test (StatView version 5.0, SAS Institute, Cary, NC, USA).

**Immunohistochemistry.** To examine cellular localization of ART3

protein in azoospermic testes, testicular biopsy specimens from 15 OA and 12 NOA patients were subjected to immunohistochemistry. Four postmortem testicular tissues of accidental sudden-deaths were used as normal controls. The testicular tissues were fixed in 10% buffered formalin and embedded in paraffin. Cryosections (3 μm thickness) were pre-incubated with the Histofine Antigen-Retrieval Solution (1:10 dilution; Nichirei Bioscience, Tokyo, Japan) for 10 minutes at 95 °C. The sections were then incubated with primary ART3 antibody (1:4,000; Abnova, Taipei, Taiwan), then with IgG2b isotype (1:4,000; MBL International, Woburn, USA) for 60 minutes at room temperature. After washing with PBS, the sections were incubated with the Histofine Simple Stain Max-PO (Multi) (1:5 dilution; Nichirei Bioscience) for 30 minutes at room temperature, and then reacted with DAB (Nichirei Bioscience) for 10 minutes at room temperature. Haematoxylin was used for counterstaining.

## Supporting Information

**Figure S1.** Statistical Analysis Reveals Transcripts Differentially Expressed among Three NOA Subclasses

Venn diagram summaries show the number of transcripts differentially expressed with significance by Tukey's *post hoc* test in each comparison (see Table S1)

Found at doi:10.1371/journal.pgen.0040026.sg001 (694 KB EPS).

**Figure S2.** Comparisons of Expression Levels of 149 Transcripts Expressed Differentially between Three NOA Subclasses in Microarray Analysis (Part I)

Natural log-transformed normalized ratios of NOA to testis reference (y-axes) were subjected to statistical analysis, as described in Materials and Methods. Each column represents mean ± standard error of the mean. The 53 transcripts with highly significant ($p < 0.01$, Tukey test) differences between the three NOA subclasses are shown in red.

Found at doi:10.1371/journal.pgen.0040026.sg002 (773 KB EPS).

**Figure S3.** Comparisons of Expression Levels of 149 Transcripts Expressed Differentially between Three NOA Subclasses in Microarray Analysis (Part II)

Natural log-transformed normalized ratios of NOA to testis reference (y-axes) were subjected to statistical analysis, as described in Materials and Methods. Each column represents mean ± standard error of the mean. The 53 transcripts with highly significant ($p < 0.01$, Tukey test) differences between the three NOA subclasses are shown in red.

Found at doi:10.1371/journal.pgen.0040026.sg003 (798 KB EPS).

**Figure S4.** Comparisons of Expression Levels of 149 Transcripts Expressed Differentially between Three NOA Subclasses in Microarray Analysis (Part III)

Natural log-transformed normalized ratios of NOA to testis reference (y-axes) were subjected to statistical analysis, as described in Materials

and Methods. Each column represents mean ± standard error of the mean. The 53 transcripts with highly significant ($p < 0.01$, Tukey test) differences between the three NOA subclasses are shown in red.

Found at doi:10.1371/journal.pgen.0040026.sg004 (822 KB EPS).

**Figure S5.** Correlations of Testicular Gene Expression Evaluated by Microarray and Quantitative Real-Time RT-PCR Analyses

Expression levels of 51 transcripts with highly significant ($p < 0.01$) differences in expression among the three NOA subclasses were quantified by real-time RT-PCR method as described in Material and Methods. Squares of correlation coefficients ($R^2$) for the respective transcripts were calculated between normalized expression ratios of NOA to testis reference in microarray data (x-axes) and the corresponding ratios obtained by real-time RT-PCR analysis (y-axes)

Found at doi:10.1371/journal.pgen.0040026.sg005 (1.7 MB EPS).

**Table S1.** 149 Transcripts Representing Statistically Significant ($p < 0.05$) Differences in Testicular Expression between Three NOA Subclasses

Found at doi:10.1371/journal.pgen.0040026.st001 (68 KB XLS).

**Table S2.** Comparison of Minor Allele Frequencies (MAFs) at 191 SNPs of 42 Genes between 190 Infertile Patients and 190 Fertile Males (First Round of Initial Screening)

Found at doi:10.1371/journal.pgen.0040026.st002 (415 KB DOC).

**Table S3.** Quantitative Real-time RT-PCR Assays for 51 Transcripts Representing Highly Significant Differences between NOA Subclasses

Found at doi:10.1371/journal.pgen.0040026.sg003 (30 KB XLS).

**References**

1. Pryor JL, Kent-First M, Muallem A, Van Bergen AH, Nolten W, et al. (1997) Microdeletions in the Y chromosome of infertile men. N Eng J Med 336: 534–539.
2. Krausz C, Rajpert-de Meys E, Frydelund-Larsen L, Quintana-Murci L, McElreavey K, et al. (2001) Double-blind Y chromosome microdeletion analysis in men with known sperm parameters and reproductive hormone profiles: microdeletions are specific for spermatogenic failure. J Clin Endocrinol Metab 86: 2638–2642.
3. Matzuk MM, Lamb DJ (2002) Genetic dissection of mammalian fertility pathways. Nat Cell Biol 4 (Supplement): S41–S49.
4. Feig C, Kirchhoff C, Ivell R, Naether O, Schulze W, et al. (2006) A new paradigm for profiling testicular gene expression during normal and disturbed human spermatogenesis. Mol Hum Reprod 13: 33–43.
5. Kim PM, Tidor B (2003) Subsystem identification through dimensionality reduction of large-scale gene expression data. Genome Res 13: 1706–1718.
6. Brunet JP, Tamayo P, Golub TR, Mesirov JP (2004) Metagenes and molecular pattern discovery using matrix factorization. Proc Natl Acad Sci U S A 101: 4164–4169.
7. Pascual-Montano A, Carmona-Saez P, Chagoyen M, Tirado F, Carazo JM, et al. (2006) bioNMF: a versatile tool for non-negative matrix factorization in biology. BMC Bioinformatics 7: 366.
8. Churchill GA (2002) Fundamentals of experimental design for cDNA microarrays. Nat Genet 32 (Supplement): 490–495.
9. Micic S (1983) The effect of the gametogenesis on serum FSH, LH and prolactin levels in infertile men. Acta Eur Fertil 14: 337–340.
10. Yaman O, Ozdiler E, Seckiner I, Gogus O (1999) Significance of serum FSH

levels and testicular morphology in infertile males. Int Urol Nephrol 31: 519–523.
11. Johnsen SG (1970) Testicular biopsy score count—a method for registration of spermatogenesis in human testes: normal values and results in 335 hypogonadal males. Hormones 1: 2–25.
12. Scanlan MJ, Simpson AJ, Old LJ (2004) The cancer/testis genes: review, standardization, and commentary. Cancer Immun 4: 1.
13. Simpson AJ, Caballero OL, Jungbluth A, Chen YT, Old LJ (2005) Cancer/testis antigens, gametogenesis and cancer. Nat Rev Cancer 5: 615–625.
14. Crackower MA, Kolas NK, Noguchi J, Sarao R, Kikuchi K, et al. (2003) Essential role of Fkbp6 in male fertility and homologous chromosome pairing in meiosis. Science 300: 1291–1295.
15. Spruck CH, de Miguel MP, Smith AP, Ryan A, Stein P, et al. (2003) Requirement of Cks2 for the first metaphase/anaphase transition of mammalian meiosis. Science 300: 647–650.
16. Greenbaum MP, Yan W, Wu MH, Lin YN, Agno JE, et al. (2006) TEX14 is essential for intercellular bridges and fertility in male mice. Proc Natl Acad Sci U S A 103: 4982–4987.
17. Hedger MP, de Kretser DM (2000) Leydig cell function and its regulation. In: McElreavey K, editor. The genetic basis of male infertility. Berlin and Heidelberg: Springer-Verlag. pp. 69–110.
18. Nagata Y, Fujita K, Banzai J, Kojima Y, Kasima K, et al. (2005) Seminal plasma inhibin-B level is a useful predictor of the success of conventional testicular sperm extraction in patients with non-obstructive azoospermia. J Obstet Gynaecol Res 31: 384–388.
19. Cheung VG, Conlin LK, Weber TM, Arcaro M, Jen KY, et al. (2002) Natural

· variation in human gene expression assessed in lymphoblastiod cells. Nat Genet 33: 422–425.

20. Morley M, Molony CM, Weber TM, Devlin JL, Ewens KG, et al. (2004). Genetic analysis of genome-wide variation in human gene expression. Nature 430: 743–747.

21. Miyamoto T, Hasuike S, Yogev L, Maduro MR, Ishikawa M, et al. (2003) Azoospermia in patients heterozygous for a mutation in SYCP3. Lancet 362: 1714–1719.

22. Kuo PL, Wang ST, Lin YM, Lin YH, Teng YN, et al. (2004) Expression profiles of the DAZ gene family in human testis with and without spermatogenic failure. Fertil Steril 81: 1034–1040.

23. Marchetti C, Hamdane M, Mitchell V, Mayo K, Devisme L, et al. (2003) Immunolocalization of inhibin and activin alpha and betaB subunits and expression of corresponding messenger RNAs in the human adult testis. Biol Reprod 68: 230–235.

24. Churchill GA, Doerge RW (1997) Empirical threshold values for quantitative trait mapping. Genetics 138: 963–971.

25. de Bakker PI, Yelensky R, Pe'er I, Gabriel SB, Daly MJ, et al. (2005) Efficiency and power in genetic association studies. Nat Genet 37: 1217–1223.

26. Stephens M, Smith NJ, Donnelly P (2001) A new statistical method for haplotype reconstruction from population data. Am J Hum Genet 68: 978–989.

27. Stephens M, Donnelly P (2003) A comparison of Bayesian methods for haplotype reconstruction from population genotype data. Am J Hum Genet 73: 1162–1169.

28. Szmulewicz M, Ruiz LM, Reategui EP, Hussini S, Herrera RJ (2002) Single-

nucleotide variant in multiple copies of a deleted in azoospermia (DAZ) sequence—a human Y chromosome quantitative polymorphism. Hum Hered 53: 8–17.

29. Vinci G, Raicu F, Popa L, Popa O, Cocos R, et al. (2005) A deletion of a novel heat shock gene on the Y chromosome associated with azoospermia. Mol Hum Reprod 11: 295–298.

30. Dieterich K, Soto Rifo R, Karen Faure A, Hennebicq S, Amar BB, et al. (2007) Homozygous mutation of AURKC yields large-headed polyploid spermatozoa and causes male infertility. Nat Genet 39: 661–665.

31. Stranger BE, Forrest MS, Clark AG, Minichiello MJ, Deutsch S, et al. (2005) Genome-wide associations of gene expression variation in humans. PLoS Genet 1: e78. doi:10.1371/journal.pgen.0010078

32. Friedrich M, Grahnert A, Paasch U, Tannapfel A, Koch-Nolte F, et al. (2006) Expression of toxin-related human mono-ADP-ribosyltransferase 3 in human testes. Asian J Androl 8: 281–287.

33. Benjamini Y, Hochberg Y (1995) Controlling the false discovery rate: a practical and powerful approach to multiple testings. J R Statist Soc B 57: 289–300.

34. Livak KJ, Schmittgen TD (2001) Analysis of relative gene expression data using real-time quantitative PCR and the $2^{-\Delta\Delta C_T}$ Method. Methods 25: 402–408.

35. Lewontin RC (1964) The interaction of selection and linkage: I. General considerations; heterotic models. Genetics 49: 49–67.

36. Hill WG, Robertson A (1968) Linkage disequilibrium in finite populations. Theor Appl Genet 38: 226–231.

37. Excoffier L, Slatkin M (1995) Maximum-likelihood estimation of molecular haplotype frequencies in a diploid population. Mol Biol Evol 12: 921–927.

# In vitro and in vivo evaluation of novel cationic liposomes utilized for cancer gene therapy

Takehiro Serikawa [a], Akira Kikuchi [a], Susumu Sugaya [a], Norio Suzuki [b], Hiroshi Kikuchi [b], Kenichi Tanaka [a,*]

[a] Department of Obstetrics and Gynecology, Niigata University Graduate School of Medical and Dental Sciences, Asahimachi-Dori, Niigata, 951-8510, Japan
[b] Drug Metabolism and Physicochemistry Research Laboratory, Daiichi Pharmaceutical Co., Ltd., Tokyo, 134-8630, Japan

## Abstract

Advanced peritoneal carcinomatoses is very difficult to treat. We have explored the potential therapeutic application of gene therapy using cationic liposomes in this disease. The lacZ gene was introduced in vitro into ovarian and endometrial cancer cells using cationic liposomes. The transfection efficiency was similar to that of commercially available liposomes in serum-free medium ($11.0–20.9\%$ vs. $5.4–26.0\%$). In serum-containing medium, the efficiency was $1.9–18.1\%$, which is comparable with the efficiency in serum-free medium. However, the efficiency of commercial liposomes decreased drastically to between $0.1\%$ and $4.7\%$ in the serum-containing medium. When cultured cells were transfected with the herpes simplex virus thymidine kinase (HSV-tk) gene and ganciclovir (GCV) was added, the anti-tumor effect of GCV was 47–640 times greater than when the same experiment was performed with lacZ gene. Evaluation of anti-tumor effect was performed with the MTT assay. In vivo, the HRA and mEIIL ascitic mice were treated with HSV-tk gene and GCV using the peritoneal route, a significant prolongation of the mean survival time was observed by Kaplan–Meier analysis (16–18 days and 15–30 days, respectively, $p<0.05$). These results indicate a potential role for gene therapy in the treatment of advanced intraperitoneal carcinomatoses using the novel cationic liposomes.
© 2006 Elsevier B.V. All rights reserved.

## 1. Introduction

The standard treatment for disseminated intraperitoneal carcinomatoses is cytoreductive surgery followed by chemotherapy. Recently, intraperitoneal hyperthermic perfusion has been increasingly investigated for intraperitoneal disease controls [1]. Even though these therapeutic modalities were well defined, improvement in the prognosis of patients with advanced intraperitoneal cancer has been disappointing. In spite of intensive clinical research, the rate presentation of patients with intraperitoneal cancer has not allowed these efforts to result in significant improvement of prognosis. Therefore, we continue to seek effective modalities of treatment that will be tolerable and easy to administer. One such treatment with great potential is gene therapy.

Gene therapy is a method that utilizes genetic manipulation in the treatment of various diseases. The concept of gene therapy involves the transfer of genetic material into a cell, tissue, or whole organ, with the goal of curing a disease or at least improving the clinical status of a patient [2], and it is one of the most hopeful strategies to date for the treatment of these previously untreatable tumors. Many studies have been performed in cancer gene therapy using various vectors [3], and remarkable progress has been reported in this field.

Herpes simplex virus thymidine kinase (HSV-tk) is one of the candidates that can be used to introduce therapeutic genes into peritoneal cancer cells [4]. The incorporation and expression of this gene in cancer cells followed by treatment with a specific prodrug, e.g. ganciclovir (GCV) is an attractive cancer gene therapy. GCV is a nontoxic nucleoside analogue, which makes it very attractive especially when one considers the toxicity associated with standard chemotherapy. This favorable profile regarding toxicity is the main reason this agent is currently

* Corresponding author. Tel.: +81 25 227 2320; fax: +81 25 227 0789.
E-mail address: tanaken@med.niigata-u.ac.jp (K. Tanaka).

undergoing intensive investigation by many researchers [5]. GCV is converted into a monophosphate form by phosphory-lation, which can be further converted into a triphosphate form by endogenous mammalian enzymes. Triphosphate-GCV changes to a toxic nucleotide analogue, which inhibits DNA replication [6].

Various vectors for gene transfer have been developed and investigated both in vitro and in vivo. However, it is difficult to find a single method that meets all the conditions for an ideal gene transfer and vector expression. There are many concerns regarding the safety of vectors and the complicated pharmaco-dynamics involved which must be resolved. Viral vectors like retroviruses and adenoviruses, which have high transgene ex-pression efficiency, have been investigated for a long time [7]. Unfortunately, they have many defects. The limitations of viral gene therapies relate to the residual viral elements within the viral vectors that can be immunogenic, cytopathic or recombi-genic [8]. Traditional nonviral chemical and physical methods such as calcium phosphate precipitation [9], administration of DEAE dextran [10] and electroporation [11] have relatively low efficiency. Furthermore, they are not well suited for in vivo use and are difficult to use for transfection of a large quantity of cells.

Cationic liposomes are nonviral vectors [12], and new de-rivatives of cationic lipid are being developed at a fast pace. Cationic liposomes are superior to viral vectors in terms of reproducibility, simplicity and safety of use. In addition, they do not invoke an immune response or protooncogene activation [13,14]. However, they are inferior to viral vectors in trans-fection efficiency. Most commercially available cationic lipo-somes were invented for in vitro rather than in vivo use, so they have low transfection efficiency under serum-containing condi-tions and are currently unsuitable for clinical use.

We previously developed and reported a series of new cationic liposomes containing $O,O'$-ditetradecanoyl-$N$-($\alpha$-trimethylam-monioacetyl) diethanolamine chloride (DC-6-14) (Fig. 1), which have transgene activities in serum-containing medium for disseminated intraperitoneal tumors [15]. In this report, we des-cribe the use of one of these novel cationic liposomes, composed of DC-6-14 and dioleoylphosphatidylethanolamine (DOPE) in a molar ratio of 5:2, for gene therapy. Furthermore, we describe its transgene expression efficiency and anti-tumor effect under serum-containing conditions. This was done in vitro but we also show significant prolongation of survival in vivo in comparison with commercially available cationic liposomes.
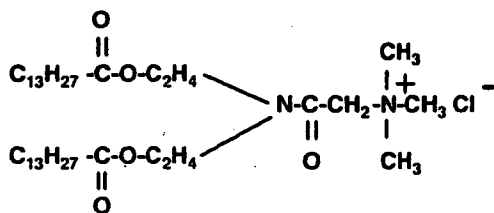


Fig. 1. Chemical structure of cationic lipid DC-6-14, $O,O'$-ditetradecanoyl-$N$-($\alpha$-trimethylammonioacetyl) diethanolamine chloride. A powerful positive charge derived from trimethylammonium gives the affinity for DNA.

## 2. Materials and methods

### 2.1. Cell lines

Six human cancer cell lines (HRA, ES-2, mEIIL, KF, SW626 and SKOV-3) were used in vitro, and two cell lines (HRA and mEIIL) were used in vivo. The HRA and KF cells were both derived from serous cystadenocarcinoma of the ovary [16,17] and were kindly provided by Dr. Yoshihiro Kikuchi (National Defense Medical College, Tokorozawa, Japan). The ES-2, SW626 and SKOV-3 cells were derived from human ovarian carcinoma [18–20] and were purchased from the American Type Culture Collection. The mEIIL (metastatic Estrogen Indepen-dent Ishikawa Line) cells were human endometrial adenocarci-noma cells [21], which were derived from the Ishikawa line [22] and were kindly provided by Dr. Hideki Sakamoto (Nihon Uni-versity, Tokyo, Japan). All six cell lines were maintained in Dulbecco's modified Eagle medium (DMEM, Immuno-Biolog-ical Laboratories, Fujioka, Japan) supplemented with 10% fetal bovine serum (FBS, JRH Biosciences, Lenexa, KS, USA).

### 2.2. Preparation of novel cationic liposomes

We prepared cationic liposomes labeled GTE-319 for gene transfer into cancer cells. DC-6-14, a positively charged lipid was purchased from Sogo Pharmaceutical Co., Ltd. (Tokyo, Japan). A powerful positive charge derived from trimethylam-monium gives the affinity for DNA. Dioleoylphosphatidyletha-nolamine (DOPE), a neutral helper lipid and essential to the formation of stable liposomes [23], was obtained from Nippon Oil and Fats (Tokyo, Japan). We prepared positively charged liposomes as mixtures with neutral helper lipids. A molar ratio of 5:2 was used for DC6-14/DOPE.

Liposomes were prepared as freeze-dried empty liposomes using a method described previously [15]. Briefly, DC6-14 and DOPE were dissolved in a chloroform–methanol mixture (4:1, v/v), and the solvent was removed in a rotary evaporator. After the lipids were mixed with 9% sucrose aqueous solution, they were hydrated at 60–70 °C and extruded through a poly-vinylidenedifluoride membrane filter with 0.22 μm pore size by using a Liponizer LP-90 (Nomura Micro Science, Kanagawa, Japan). The dispersion was pipetted into glass vials (0.5 or 2 ml portion each) and lyophilized in a freeze-drier (Virtis, NY, USA). The dried liposomes were then reconstituted with 0.5 or 2 ml of distilled water by a gentle mixing prior to transfection.

As a control, we used the commercially available cationic liposomes DMRIE-C and LipofectAMINE (Life Technologies, Inc., Rockville, MD, USA).

### 2.3. Construction of expression plasmids

Dr. Jun-ichi Miyazaki (Osaka University, Osaka) generously provided the expression plasmid pCAG-lacZ. The pCAG vector expresses an inserted DNA by its CAG promoter, which con-sists of the cytomegalovirus immediate early enhancer sequence and the chicken β-actin/rabbit β-globin hybrid promoter [24]. The HSV-tk gene was derived from plasmid pHSV-106 (Life

Technologies, Inc.) [25] by polymerase chain reaction (PCR) amplification using the primers 5'-GCC-CGA-ATT-CTA-GAA-GCG-CGT-ATG-GCT-TCG-3' (sense) and 5'-CCG-CGA-ATT-CCC-GTG-TTT-CAG-TTA-GCC-TCC-3' (anti-sense). The PCR products were purified by a Microspin S-400HR column (Pharmacia Biotech, Tokyo, Japan) after digestion with EcoRI. The lacZ gene of the pCAG-lacZ was removed by digestion with EcoRI. We designed the pCAG-HSVtk plasmid, which was constructed by replacing the lacZ gene in the pCAG-lacZ with the HSV-tk cDNA fragment.

### 2.4. In vitro transfer of the lacZ gene and X-Gal staining

Cells were seeded on 6-well plates (Corning-Coaster, Cambridge, MA, USA) and incubated to reach about 30–50% confluence at 37 °C in 5% $CO_2$. One hundred microliters of serum-free DMEM containing 1 μg of the lacZ gene was mixed with 100 μl of serum-free DMEM containing an appropriate amount of GTE-319 suspensions (10 nmol of DC-6-14), DMRIE-C suspensions (10 nmol of DMLIE: 1,2-dimyristyloxypropyl-3-dimethyl-hydroxy ethyl ammonium bromide) or LipofectA-MINE suspensions (5 nmol of DOSPA: 2.3-dioleyloxy-N-[2 (spermine carboxyamido) ethyl]-N,N-dimethyl-1-propanami-niumtrifluoroacetate) with mild agitation in polystyrene tubes and incubated for 15 min at room temperature. Prior to transfection, 800 μl of DMEM containing 12.5% FBS (final conc. 10% FBS) were added. Transfection was also performed under serum-free conditions. Cells were washed with serum-free medium and added to 1 ml of liposomes/plasmid complexes. After 5-h incubation at 37 °C, the old medium was removed, then cells were washed, added to serum-containing medium and cultured for 48 h. To evaluate transfection efficiency, 5-bromo-4-chloro-3-iodolyl β-D-galactoside (X-Gal, Life Technologies, Inc.) staining assay was performed as previously described elsewhere [26]. Percentages of lacZ expression cells were determined by counting at least 1000 cells with a microscope.

### 2.5. In vitro sensitivity to GCV

To evaluate the effect of the HSV-tk gene transfection with GTE-319 and GCV administration in vitro, the cells were seeded on 96-well plates (Greiner Labortechnik GmbH, Frickenhausen, Germany) at $1-3 \times 10^3$ cells per 80 μl of DMEM containing 12.5% FBS and incubated for 24 h. An equal volume of the lacZ gene or the HSV-tk gene (1–10 μg/ml in serum-free DMEM) and GTE-319 suspensions (cationic lipid 10–100 nmol/ in serum-free DMEM) were mixed and incubated for 15 min at room temperature. Twenty microliters of liposomes/plasmid complexes was added to each well. After 5 h of incubation at 37 °C, the old medium was aspirated with a 23-gauge needle, and 200 μl of DMEM containing 10% FBS with 0, 0.001, 0.01, 0.1, 1, 10, 100 and 1000 μg/ml of GCV were added to each well. For evaluation of the anti-tumor effect in vitro, MTT assay was performed [27] after 96–144-h incubation. The IC50 value was determined by extrapolation and detailed graphically. The therapeutic index was determined by comparing the IC50 values of the lacZ gene-treated cells and HSV-tk gene-treated cells (lacZ IC50/HSV-tk IC50).

### 2.6. Animals

Five-week-old female CD-1 nu/nu athymic nude mice weighing 20–30 g were purchased from Charles River Japan (Yokohama, Japan) and maintained in a specific pathogen-free environment. When necessary, the animals were killed or their ascites was aspirated from their peritoneal cavities.

### 2.7. In vivo transfer of the lacZ gene and X-Gal staining

Viable HRA cells, $6 \times 10^7$ in 1 ml of DMEM containing 10% FBS, were inoculated into intraperitoneal cavities of nude mice with a 26-gauge needle. Two days after HRA cell inoculation, the pCAG-lacZ was transferred into cancer cells in the peritoneal cavity. Five hundred microliters of serum-free DMEM containing 20μg of the pCAG-lacZ was mixed with 500 μl of serum-free DMEM containing 200 nmol of GTE-319 suspension and incubated for 2 min at room temperature, and then mice were injected with 1 ml of the liposomes/plasmid complexes. Twenty-four hours later, we injected saline into the intraperitoneal cavity and ascites were aspirated from the mice intraperitoneal cavities. To remove red blood cells, the pellets were suspended in 0.15 M $NH_4Cl-1$ mM KCL-0.1 mM $Na_2EDTA$, pH 7.4 after centrifugation at 1000 rpm for 5 min. Then $3 \times 10^5$ HRA cells were seeded onto 6-well plates and incubated for 24 h. X-Gal staining was performed the same as in the in vitro experiment.

### 2.8. Intraperitoneal transfection of the HSV-tk and the lacZ gene to the nude mice and GCV administration

Viable HRA cells, $3 \times 10^5$, and $5 \times 10^6$ mEIIL cells in 1 ml of DMEM containing 10% FBS were inoculated into the peritoneal cavities of nude mice with a 26-gauge needle. The mice were

**(A)**

HRA $(3 \times 10^5)$

GCV 35 mg/kg × 2 / everyday i.p.(Days 9-21)

liposomes / plasmid complexes i.p.

D0    D7 D9 D11 D13 D15 D17 D19 D21

**(B)**

mEIIL $(5 \times 10^6)$

GCV 35 mg/kg × 2 / everyday i.p.(Days 12-24)

liposomes / plasmid complexes i.p.
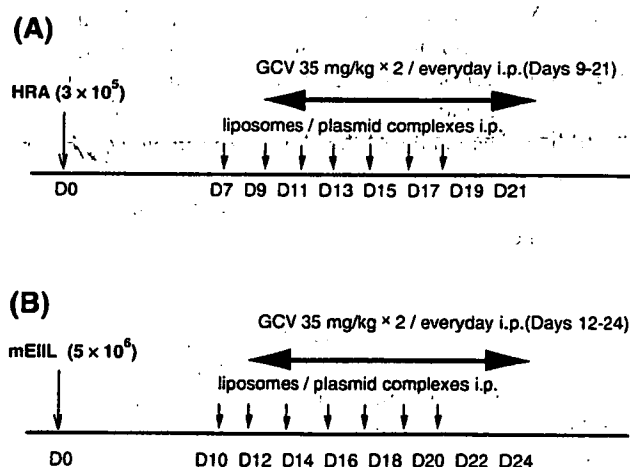
D0    D10 D12 D14 D16 D18 D20 D22 D24

Fig. 2. Protocol of the transfection and GCV treatment of malignant cells disseminated in the mouse peritoneal cavity. (A) After HRA cells were inoculated on day 0, liposomes/plasmid complexes were injected i.p. every 2 days from day 7 to day 19 and GCV was injected i.p. twice a day from day 9 to day 21. (B) After mEIIL cells were inoculated on day 0, liposomes/plasmid complexes were injected i.p. every 2 days from day 12 to day 24 and GCV was injected i.p. twice a day from day 14 to day 26.

Table 1

In vitro transfection efficiency cells in the presence or absence of serum

| Cell line | Transfection efficiency (%) | | | | | |
|-----------|------|------|------|------|------|------|
| | Serum (−) | | | Serum (+) | | |
| | GTE-319 | DMRIE-C | LipofectAMINE | GTE-319 | DMRIE-C | LipofectAMINE |
| HRA | 20.9 | 9.6 | 11.8 | 9.1 | 1.3 | 4.7 |
| mEIIL | 11.0 | 12.6 | 20.5 | 4.4 | 4.0 | 0.6 |
| ES-2 | 17.3 | 17.7 | 26.0 | 13.1 | 10.1 | 3.3 |
| KF | 12.9 | 9.4 | 16.1 | 9.4 | 0.6 | 0.1 |
| SKOV-3 | 17.4 | 13.1 | 5.4 | 1.9 | 0.2 | 0.1 |
| SW626 | 16.8 | 9.5 | 17.9 | 18.1 | 4.2 | 0.2 |

divided into two groups: the HSV-tk treatment group and the lacZ treatment group. Seven days after HRA cell inoculation (Fig. 2A) and 10 days after mEIIL cell inoculation (Fig. 2B), gene therapy was started. Twenty micrograms of plasmid in 500 μl of serum-free DMEM and 200 nmol of cationic lipid in 500 μl of serum-free DMEM were gently mixed. One milliliter of liposomes/plasmid complexes was injected i.p. every 2 days seven times. Intraperitoneal injections of GCV (35 mg/kg) were performed twice a day for 13 days starting 2 days after the first injection of liposomes/plasmid complexes. The animals' body weight was measured every 3 days during GCV treatment, and animals were observed daily until death. Results are represented by the Kaplan–Meier method. The Wilcoxson method was used for statistical analysis.

## 3. Results

### 3.1. Transfection efficiencies of the lacZ gene in vitro

Liposomes/plasmid complexes were transferred into the cells in the absence or presence of serum 24 h after the cell had been seeded to a 6-well plate. Forty-eight hours after transfection of the lacZ gene in the absence or presence of 10% FBS, we performed X-Gal staining. Under a microscope, the lacZ gene expression cells appeared to be made of blue cytoplasm. We evaluated transfection efficiency by counting the percentages of blue-dyed cells, and at least 1000 cells were counted from each cell line. The results of the above experiment are shown in Table 1, and data represent the means of three experiments.

In the absence of serum, both commercially available cationic liposomes and GTE-319 showed comparable high expression efficiency: 11.0–20.9% in GTE-319, 9.4–17.7% in DMRIE-C and 5.4–26.0% in LipofectAMINE in all six cell lines. In the presence of 10% serum, the transfection efficiency of GTE-319 was more effective (1.9–18.1% efficiency) than that of commercially available cationic liposome reagents, which showed a marked decrease of transfection efficiency: 1.3–10.1% in DMRIE-C and 0.1–4.7% in LipofectAMINE.

### 3.2. In vitro sensitivity to GCV

In the case of the cells transferred with pCAG-HSVtk plasmid in the presence of 10% FBS, the IC50 values of GCV for HRA, mEIIL, ES-2, KF, SKOV-3 and SW626 cells were 0.025,

1.3, 0.062, 0.284, 3.8 and 2.05 μg/ml, respectively. In contrast, in the case of the pCAG-lacZ-transfected cells, the IC50 values of GCV for HRA, mEIIL, ES-2, KF, SKOV-3 and SW626 cells were 16, 62, 6.2, 25.5, 490 and 96 μg/ml, respectively. This is summarized in Table 2. The cells transfected with the HSV-tk gene had 640, 48, 100, 90, 129 and 47, respectively, times as much sensitivity as the cells transfected with the lacZ gene. What is evident from the table is that suicidal gene therapy by the HSV-tk/GCV system using our novel cationic liposomes was an effective method for treatment of malignant cells in vitro.

### 3.3. Transfection efficiencies of the lacZ gene in vivo

The methods detailed in Materials and methods determined the percentages of transfection efficiency. The percentage of lacZ-positive cells in HRA was $4.4 \pm 1.0\%$ ($n=3$). Transfection efficiency in vivo was about half of the efficiency achieved in vitro.

### 3.4. Prolongation of survival of animals with intraperitoneal injection of the HSV-tk gene and GCV

HRA ascitic mice ($n=12$) were followed for 70 days, and the mean survival of the HSV-tk gene/GCV-treated group and the lacZ gene/GCV-treated group was 51.6 and 35.6 days, respectively. Kaplan–Meier survival curves are shown in Fig. 3A. The mEIIL ascitic mice ($n=8$) were followed for 85 days, and the mean survival of the HSV-tk gene/GCV-treated group and the lacZ gene/GCV-treated group were 76.9 and 62.1 days, respectively (Fig. 3B). In both cell lines, the mean survival of the HSV-tk treatment group was significantly

Table 2

In vitro sensitivity of cancer cells introduced by the HSV-tk gene to GCV

| Cell line | HSV-tk | lacZ | Therapeutic index |
|-----------|--------|------|-------------------|
| | IC50 (μg/ml) | | |
| HRA | 0.025 | 16 | 640 |
| mEIIL | 1.3 | 62 | 48 |
| ES-2 | 0.062 | 6.2 | 100 |
| KF | 0.284 | 25.5 | 90 |
| SKOV-3 | 3.8 | 490 | 129 |
| SW626 | 2.05 | 96 | 47 |

**(A) HRA**



Days after HRA cells inoculation

**(B) mEIIL**



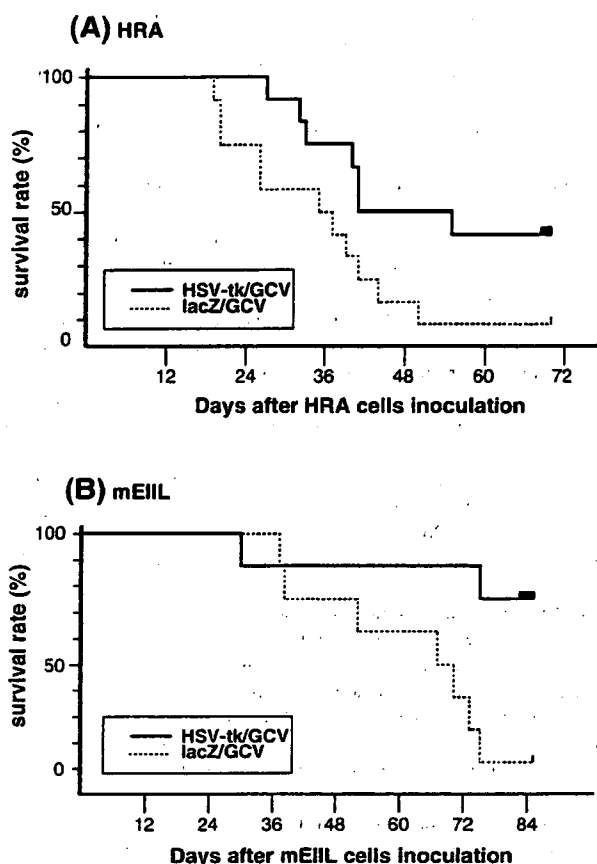Days after mEIIL cells inoculation

Fig. 3. Kaplan–Meier analysis of the survival of animals with HSV-tk gene/GCV (continuous line), with the lacZ/GCV (interrupted line) and without treatment (dotted line). (A) Inoculated HRA cells ($n$=12). The survival rate of the HSV-tk treatment group was significantly high compared with the lacZ-treated group ($p$<0.05). (B) Inoculated mEIIL cells ($n$=8). The rate was higher in the HSV-tk treatment group than in the lacZ treatment group ($p$<0.05).

longer than that of the lacZ treatment group ($p$<0.05, Wilcoxson test).

## 4. Discussion

Recently, several nonviral delivery and expression systems of exogenous genes into culture cells in vitro and different internal organs in vivo have been developed [8,28]. One of these is the cationic lipid-based system, which utilizes cationic liposomes. This system meets the requirements for efficiency, safety and repetition [23]. Cationic liposomes have numerous advantages when compared to other nonviral vectors; the technique is simple, highly reproducible and more efficient than some commonly used techniques [12]. Several clinical trials for gene therapy using cationic liposomes are ongoing with human genetic diseases and cancer. Initial results from these trials are encouraging [29].

In general, cationic liposomal transfection efficiency is reduced in the presence of serum [12,14,23]. Serum contains various types of charged molecules, which may bind to liposomes. Thereby this modification renders structural and physi-

cal characteristics of the cells sensitive to nucleases. For this reason, new cationic liposomes, which have an ideal formulation and good transgene efficiency under serum-containing conditions, have been developed for clinical use [15,30].

We developed cationic liposomes based on DC-6-14 for efficient gene transfer into peritoneally disseminated tumors. DC-6-14 has unique properties for gene delivery into human cancer cells in serum-containing medium. In the present study, the lacZ gene was transferred to human cancer cells with GTE-319 based on DC-6-14 and commercially available cationic liposomes in serum-free or serum-containing medium in vitro.

The transfection efficiency of GTE-319 was similar to other commercially available cationic liposomes for all cancer cells in the serum-free condition (Table 1). In the experiment on transgene expression through commercially available liposomes, the transfection efficiency was reduced by the presence of serum. By contrast, transgene expression using GTE-319 was maintained in serum-containing medium. Thus, GTE-319 was 1.1- to 15.7-fold more effective than DMRIE-C and 1.9- to 94.0-fold more effective than LipofectAMINE in all six cell lines in the presence of 10% serum (Table 1). These results showed that these cationic liposomes demonstrated a consistently superior transfection efficiency in the presence of serum in vitro. Therefore, the use of GTE-319 would be advantageous for clinical use in human cancer therapy.

To evaluate the anti-tumor effect of GTE-319 based on DC-6-14 in vitro, MTT assay was performed and the IC50 values of GCV were determined graphically. As shown in Table 2, the IC50 values of GCV for the lacZ gene transfection cells (therapeutic index) were 640-, 48-, 100-, 90-, 129- and 47-fold higher than those for the HSV-tk gene transfection cells of HRA, mEIIL, ES-2, KF, SKOV-3 and SW626, respectively. Our inference from this result is that HSV-tk/GCV suicidal gene therapy with GTE-319 liposomes was effective for treating cancer cells in vitro. Although transgene expression efficiency was generally low in vitro (1.9% to 18.1%, Table 1), malignant cells were killed by low concentrations of GCV. This phenomenon was probably due to the so-called bystander effect. Bystander effect describes a situation where neighboring cells suffer toxicity even though they are not genetically modification. The mechanism involved is poorly understood. It may require cell–cell contact via gap junction [31].

In this experiment, even though transfection efficiency was almost the same between cell lines (for example, HRA: 9.1%, KF: 9.4%), a difference was observed in therapeutic index (HRA: 640, KF: 90). This scenario may indicate differences in the level of gap junction expression by individual cell. Moreover, different sensitivities of cells to phosphated GCV mimic the clinical situation where different histological types of cancer have different sensitivities to anticancer chemotherapy. These possibilities will have to be explored.

Following confirmation of adequate therapeutic effect of gene therapy in six different cancer cell lines in vitro, we proceeded to evaluate gene therapy on HRA and mEIIL ascitic mice. We used survival time to evaluate in vivo anti-tumor effects. Although transfection efficiency was low in HRA cells (4.4%), we found that suicidal gene therapy using GTE-319

significantly prolonged survival of the two kinds of ascitic mice (Fig. 3). Part of the observed therapeutic effect may also be due to the phenomenon of bystander effect in vivo.

Although more researches still needed in this area, our findings are very encouraging and we feel that our approach has potential therapeutic application in the management of cancer.

## Acknowledgements

## References

[1] B.W. Loggie, R.A. Fleming, R.P. Mcquellon, G.B. Russell, K.R. Geisinger, Cytoreductive surgery with intraperitoneal hyperthermic chemotherapy for disseminated peritoneal cancer of gastrointestinal origin, Am. Surg. 66 (2000) 561–568.

[2] I.M. Verma, M.D. Weitzman, Gene therapy: twenty-first century medicine, Ann. Rev. Biochem. 74 (2005) 711–738.

[3] T. Yoshida, S. Ohnami, K. Aoki, Development of gene therapy to target pancreatic cancer, Cancer Sci. 95 (2004) 283–289.

[4] C. Lechanteur, P. Delvenne, F. Princen, M. Lopez, G. Fillet, J. Gielen, M.P. Merville, 'V. Bours, Combined suicide and cytokine gene therapy for peritoneal carcinomatosis, Gut 14 (2000) 343–348.

[5] C. Denning, J.D. Pitts, Bystander effects of different enzyme-prodrug system for cancer gene therapy depend on different pathways for intracellular transfer of toxic metabolites, a factor that will govern clinical choice of appropriate regimes, Hum. Gene Ther. 8 (1997) 1825–1835.

[6] M.C. Esandi, G.D. Van Someren, A.J.P.E. Vincent, D.W. Van Bekkum, D. Valerio, A. Bout, J.L. Noteboom, Gene therapy of experimental malignant mesothelioma using adenovirus vectors encoding the HSVtk gene, Gene Ther. 4 (1997) 280–287.

[7] N. Wu, M.M. Ataai, Production of viral vectors for gene therapy applications, Curr. Opin. Biotechnol. 11 (2000) 205–208.

[8] F.D. Ledley, Nonviral gene therapy: the promise of genes as pharmaceutical products, Hum. Gene Ther. 6 (1995) 1129–1144.

[9] M. Wigler, S. Silverstein, L.S. Lee, A. Pellicer, Y.C. Cheng, R. Axel, Transfer of purified herpes virus thymidine kinase gene to cultured mouse cell, Cell 11 (1977) 223–232.

[10] Y. Ishikawa, C.J. Homcy, High efficiency gene transfer into mammalian cells by a double transfection protocol, Nucleic Acids Res. 20 (1992) 4367.

[11] L. Paquereau, A.L. Cam, Electroporation-mediated gene transfer into hepatocytes: preservation of a growth hormone response, Anal. Biochem. 204 (1992) 147–151.

[12] P.L. Felgner, T.R. Gadek, M. Holm, R. Roman, H.W. Chan, M. Wenz, J.P. Northrop, G.M. Ringold, Lipofectin: a highly efficient, lipid-mediated DNA-transfection procedure, Proc. Natl. Acad. Sci. U. S. A. 84 (1987) 7413–7417.

[13] J. Zabner, A.I.J. Fasbender, T. Moninger, K.A. Poellinger, Cellular and molecular barriers to gene transfer by a cationic lipid, J. Biol. Chem. 270 (1995) 18997–19007.

[14] P.L. Felgner, G.M. Ringold, Cationic liposome-mediated transfection, Nature 337 (1989) 387–388.

[15] A. Kikuchi, Y. Aoki, S. Sugaya, T. Serikawa, K. Takakuwa, K. Tanaka, N. Suzuki, H. Kikuchi, Development of novel cationic liposomes for efficient gene transfer into peritoneal disseminated tumor, Hum. Gene Ther. 10 (1999) 947–955.

[16] Y. Kikuchi, I. Kizawa, K. Oomori, et al., Establishment of a human ovarian cancer cell line capable of forming ascites in nude mice and effects of tranexamic acid on cell proliferation and ascites formation, Cancer Res. 47 (1987) 592–596.

[17] Y. Kikuchi, I. Iwano, K. Kato, Effects of calmodulin antagonists on human ovarian cancer cell proliferation in vitro, Biochem. Biophys. Res. Commun. 123 (1984) 385–392.

[18] D.H.M. Lau, K.L. Ross, B.I. Sikic, Paradoxical increase in DNA cross-linking in a human ovarian carcinoma cell line resistant to cyanomorpholino doxorubicin, Cancer Res. 50 (1990) 4056–4060.

[19] J. Fogh, W.C. Wright, J.D. Loveless, Absence of HeLa cell contamination in 169 cell lines derived from human tumors, J. Natl. Cancer Inst. 58 (1977) 209–214.

[20] J. Fogh, J.M. Fogh, T. Orfeo, One hundred and twenty-seven cultured human tumor cell lines producing tumors in nude mice, J. Natl. Cancer Inst. 59 (1977) 221–226.

[21] H. Sakamoto, X. Deng, T. Shirakawa, S. Ige, K. Ohtani, A. Saitoh, M. Takami, K. Satoh, Establishment of metastatic sub-clone from estrogen independent Ishikawa cells and its characterization in vitro and in vivo, Acta Obstet. Gynaecol. Jpn. 47 (1995) 249–256.

[22] M. Nishida, K. Kasahara, M. Kaneko, H. Iwasaki, Establishment of a new human endometrial adenocarcinoma cell line, Ishikawa cells, containing estrogen and progesterone receptors, Acta Obstet. Gynaecol. Jpn. 37 (1985) 1103–1111.

[23] X. Gao, L. Huang, Cationic liposome-mediated gene transfer, Gene Ther. 2 (1995) 710–722.

[24] H. Niwa, K. Yamamura, J. Miyazaki, Efficient selection for high-expression transfectants with a novel eukaryotic vector, Gene 108 (1991) 193–200.

[25] S.L. Mcknight, E.R. Gavis, Expression of the herpes thymidine kinase gene in Xenopus laevis oocytes: an assay for the study of deletion mutants constructed in vivo, Nucleic Acids Res. 8 (1980) 5931–5948.

[26] S. Sugaya, K. Fujita, A. Kikuchi, H. Ueda, K. Takakuwa, S. Kodama, K. Tanaka, Inhibition of tumor growth by direct intratumoral gene transfer of herpes simplex virus thymidine kinase gene with DNA-liposome complexes, Hum. Gene Ther. 7 (1996) 223–230.

[27] F. Denizot, R. Lang, Rapid colorimetric assay for cell growth and survival. Modifications to the tetrazolium dye procedure giving improved sensitivity and reliability, J. Immunol. Methods 87 (1986) 271–277.

[28] S. Li, L. Huang, Nonviral gene therapy: promises and challenges, Gene Ther. 7 (2000) 31–34.

[29] S.C. Hyde, K.W. Southern, U. Gileadi, E.M. Fitzjohn, K.A. Mofford, B.E. Waddell, H.C. Gooi, C.A. Goddard, K. Hannavy, S.E. Smyth, J.J. Egan, F.L. Sorgi, L. Huang, A.W. Cuthbert, M.J. Evans, W.H. Colledge, C.F. Higgins, A.K. Webb, D.R. Gill, Repeat administration of DNA/liposomes to the nasal epithelium of patients with cystic fibrosis, Gene Ther. 7 (2000) 1156–1165.

[30] T. Serikawa, N. Suzuki, H. Kikuchi, K. Tanaka, T. Kitagawa, A new cationic liposome for efficient gene delivery with serum into cultured human cells: a quantitative analysis using two independent fluorescent probes, Biochim. Biophys. Acta 1467 (2000) 419–430.

[31] M. Mesnil, H. Yamasaki, Bystander effect in herpes simplex virus-thymidine kinase/ganciclovir cancer gene therapy: role of gap-junctional intercellular communication, Cancer Res. 60 (2000) 3989–3999.

ELSEVIER

Case Report

# Advanced malignant rhabdoid tumor of the ovary effectively responding to chemotherapy: A case report and review of the literature

Chiaki Banzai [a], Tetsuro Yahata [a,*], Jun Sasahara [a], Katsunori Kashima [a], Kazuyuki Fujita [a], Ken Nishikura [b], Yoichi Ajioka [b], Teiichi Motoyama [c], Kenichi Tanaka [a]

[a] Division of Obstetrics and Gynecology, Department of Cellular Function, Niigata University, Graduate School of Medical and Dental Sciences, Niigata, Japan
[b] Division of Molecular and Functional Pathology, Department of Cellular Function, Niigata University,
Graduate School of Medical and Dental Sciences, Niigata, Japan
[c] Department of Pathology, Yamagata University School of Medicine, Yamagata, Japan

## Abstract

Background. Malignant rhabdoid tumors (MRTs) are highly malignant neoplasms that consist of both renal and extrarenal subtypes. Primary ovarian cases are extremely rare. We herein describe the third known case of ovarian origin, which effectively responded to combination chemotherapy with ifosfamide, epirubicin, and cisplatin (IEP chemotherapy).

Case. A 19-year-old woman was diagnosed to have stage IIIc primary MRT of the ovary following the resection of tumors. Two months after surgery, an 8 cm-sized pelvic mass and enlarged retroperitoneal lymphnodes were detected. The patient received intravenous tri-weekly IEP chemotherapy. After the second course of chemotherapy, she demonstrated a complete clinical response.

Conclusion. Although this type of tumor is quite aggressive and chemotherapy is generally not considered to be effective, IEP chemotherapy may be useful in the treatment of MRT of the ovary.
© 2007 Elsevier Inc. All rights reserved.

Keywords: Malignant rhabdoid tumor; IEP chemotherapy

## Introduction

Malignant rhabdoid tumors (MRTs), consisting of renal and extrarenal rhabdoid tumors, are uncommon and have an extremely poor prognosis due to their rapid growth and tendency to metastasize early. Extrarenal rhabdoid tumor has been reported to occur in various sites throughout the body. The most common site of extrarenal rhabdoid tumors is the central nervous system, whereas ovarian cases are extremely rare with only two previous case report [1,2]. These tumors are aggressive and respond poorly to therapy. In general, chemotherapy does not appear to be effective and only a surgical extirpation is considered to offer a chance for controlling this disease. We herein describe the third patient with MRT of the ovary, who effectively responded to chemotherapy with ifosfamide, epirubicin, and cisplatin.

## Case report

A 19-year-old gravida 0 para 0 woman presented with a 2-month history of abdominal distension. A pelvic examination revealed a large pelvic mass and an abdominal computed tomographic (CT) scan and magnetic resonance image showed a 14×12×10 cm sized lobulated mass in the pelvic cavity with massive ascites. Her laboratory studies including tumor markers, AFP, CEA, CA19-9, and SCC, were all within normal limits except elevated CA125 level (875 U/ml). During the operation, a solid right ovarian tumor, measuring 14 cm in diameter, and enlarged paraaortic lymphnodes were noted. The left ovary, uterus, omentum, and pelvic lymphnodes were unremarkable. The patient underwent an abdominal total hysterectomy,

* Corresponding author. Department of Obstetrics and Gynecology, Niigata University School of Medicine, 1-757 Asahimachi-dori, Niigata 951-8510, Japan. Fax: +81 25 227 0789.
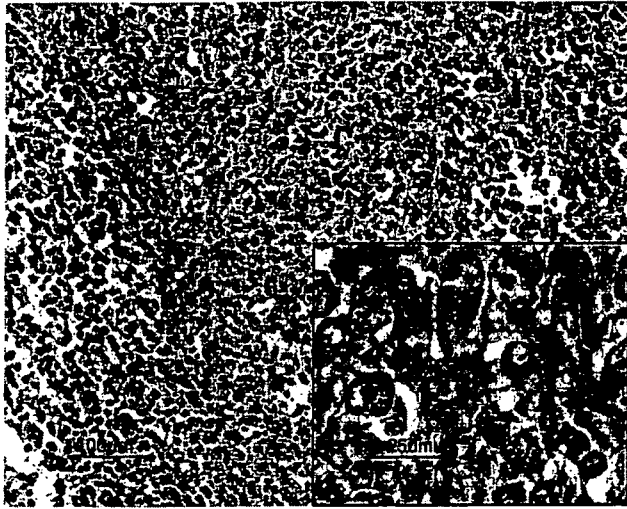E-mail address: yahatat@med.niigata-u.ac.jp (T. Yahata).

Fig. 1. Histopathology slide of the ovarian tumor showing diffusely infiltrating tumor cells in sheet-like alveolar structure (hematoxylin and eosin stain, original magnification ×100). The tumor is composed of round-shaped to pleomorphic atypical cells demonstrating large nuclei with prominent nucleoli (inset, original magnification ×400).

bilateral salpingo-oophorectomy, and pelvic and paraaortic lymphadenectomy. Intraoperative pelvic washing cytology was positive. Although the tumors were completely resected, metastasis to the paraaortic lymphnode was confirmed by postoperative histology and she was thus diagnosed to have stage IIIc ovarian carcinoma.

A histologic examination revealed a right ovarian tumor consistent with a malignant rhabdoid tumor (Fig. 1). The tumor is composed of round-shaped to pleomorphic atypical cells demonstrating large nuclei with prominent nucleoli, and abundant eosinophilic cytoplasm in which hyaline globular inclusions are conspicuously associated. Mitotic figures are frequently observed and lymphatic permeation is moderately observed. An immunohistochemical study revealed the tumor cells to be diffusely immunoreactive for vimentin, a common mesenchymal marker, and focally positive for cytokeratin markers, CAM5.2 (mixture of CK8, 18, and 19) and AE1/AE3 (mixture of CK1 to 8, 10, 14, 15, 16, and 19). No tumor cells were immunoreactive for striated muscular markers (HHF3.5, MyoD1, Myogenin, Myoglobin) or smooth muscular markers (HHF35, SMA, Desmin).
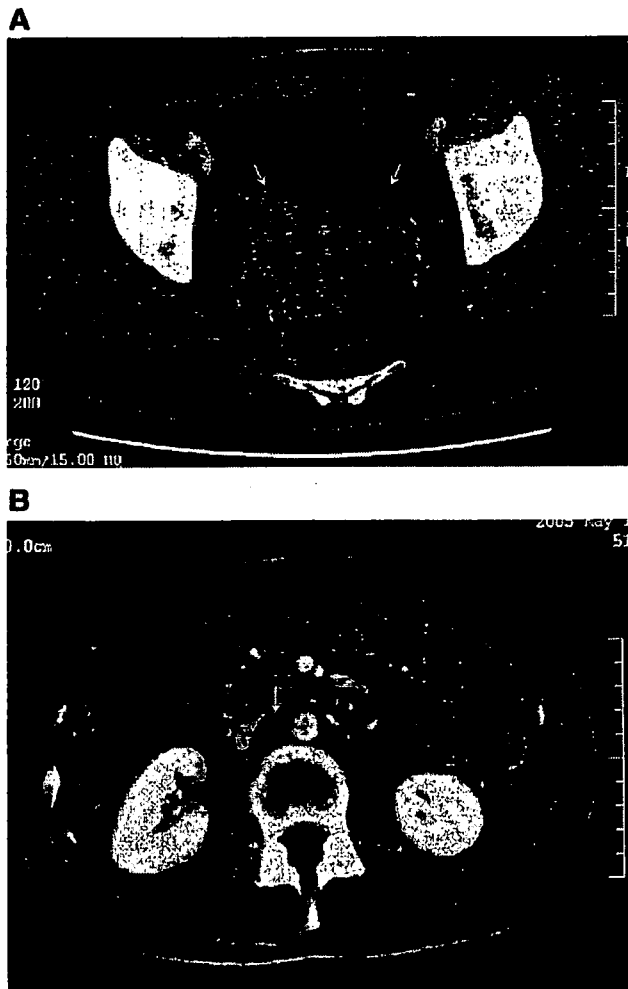


Fig. 2. CT scans showing a pelvic mass and paraaortic lymphnode swelling before IEP chemotherapy. (A) The 8 cm sized pelvic mass (white arrows) (B) and swelling of the paraaortic lymphnode (white arrow).
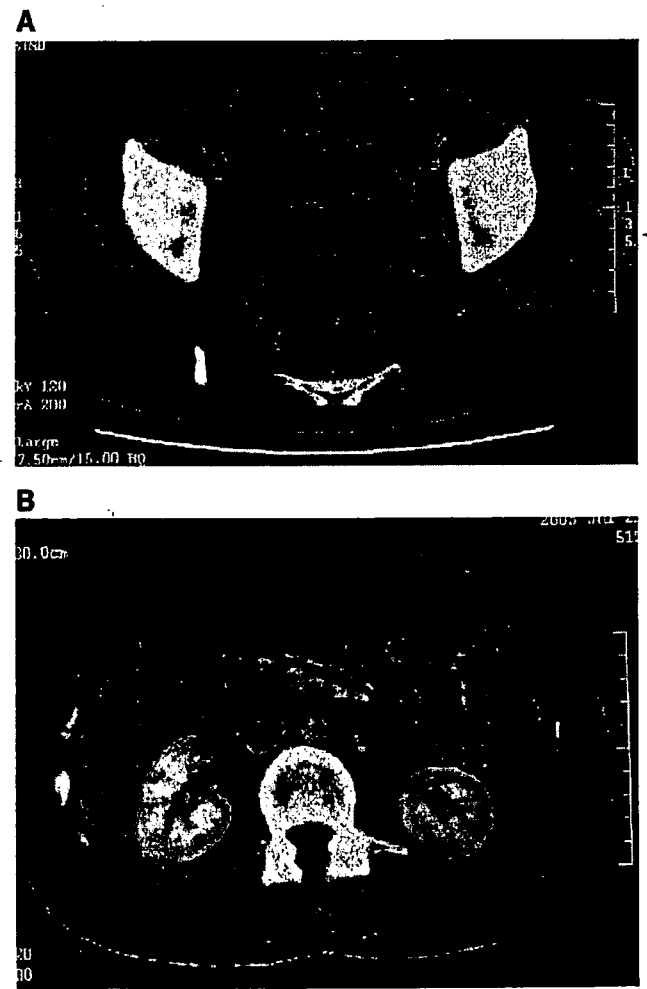


Fig. 3. CT scans after a second course of IEP chemotherapy. (A) The pelvic mass completely disappeared. (B) The swelling of paraaortic lymphnode completely resolved.

Although no consistently effective regimen for MRT has yet been reported, we decided to initiate adjuvant chemotherapy because the case was advanced with extremely poor prognosis. Finally, the patient and her family decided not to have adjuvant chemotherapy and instead requested careful observation for any recurrence. Two months after surgery, an abdominal and pelvic CT scan showed an 8 cm-sized pelvic mass, enlarged paraaortic and right internal iliac lymphnodes, and small disseminated masses in the abdomen (Figs. 2A, B). The treatment was initiated with intravenous tri-weekly IEP chemotherapy (ifosfamide (1.5 g/body × 5 days), epirubicin (50 mg/m$^2$ × 1 day), and cisplatin (70 mg/m$^2$ × 1 day)). After the first course of IEP chemotherapy, the pelvic tumor decreased by −30%. After the second course, an abdominal and pelvic CT scan showed a complete resolution of the recurrent pelvic tumor, lymphnodes, and peritoneal dissemination (Figs. 3A, B). The CA125 level

Table 1
Malignant rhabdoid tumors of the female genital tract: summary of the reported cases

| Case | Primary site | Age | Surgery | Stage | Site of metastasis at diagnosis | Recurrence (site (months after surgery)) | Chemotherapy Regimen | Response | Radiation Response | Prognosis | Reference |
|---|---|---|---|---|---|---|---|---|---|---|---|
| 1 | Vulva | 19 | Radical resection, ILD | I | – | Vulva (26 m) | – | – | – | NED (38 m) | Perrone |
| 2 | Vulva | 31 | Wide local excision, ILD | I | – | Vulva, lung, liver, retroperitoneal node (35 m) | Adriamycin, cytoxan, vincristine, dacarbazine | PD | SD | DOD (11 years) | Perrone |
| 3 | Vulva | 25 | Excision | II | – | – | Regimen: NA | NE | – | NED (8 m) | Igarashi |
| 4 | Vulva | 30 | Wide local excision | II | – | Vulva, lung (2 m) | Adriamycin | PR | – | DOD (8 m) | Perrone |
| 5 | Vulva | 39 | Radical resection, ILD | II | – | Inguinal, pelvic, paraaortic lymphnode (3 m) | Cisplatin, etoposide | PD | PD | DOD (6 m) | Lupi |
| 6 | Vulva | 40 | Local excision | II | – | Vulva (1 m) | – | – | NE | NED (61 m) | Brand |
| 7 | Vulva | 49 | Local excision | II | – | Vulva, pubis (1 m) | Regimen: NA | NA | – | DOD (9 m) | Matias |
| 8 | Vulva | 63 | Radical resection, ILD | II | – | – | – | – | NE | NED (30 m) | Tzilinis |
| 9 | Vulva | 44 | Radical resection | IVb | Inguinal lymphnode, lung | Vulva, inguinal lymphnode (2 m) | Etoposide | PD | NE | DOD (7 m) | Sert |
| 10 | Uterine body | 39 | TAH, BSO, PLN, PAN | Ic | – | Lung, liver, abdomen (12 m) | – | – | NE | DOD (17 m) | Cattani |
| 11 | Uterine body | 49 | TAH, BSO | IIIb | Dougras pouch, vagina | Peritoneum, liver (3 m) | – | – | PD | DOD (4 m) | Gaetner |
| 12 | Uterine body | 37 | TAH, BSO, PLN, PAN | IIIc | Ovary, pelvic and paraaortic nodes | Abdomen, paraaortic lymphnode (2 m) | Cisplatin | PD | – | DOD (4 m) | Hseuh |
| 13 | Uterine body | 46 | TAH, BSO | IVb | Lung, liver | Vagina (1 m) | Ifosfamide, adriamycin, etoposide, vincristine, cyclophosfamide | NA | – | DOD (<12 m) | Cho |
| 14 | Uterine body | 56 | TAH, BSO, tumor debulking | IVb | Pelvic wall, sigmoid colon, omentum | – | Ifosfamide, etoposide | NA | – | Alive (7 m) | Niemann |
| 15 | Uterine body | 72 | SH, BSO, tumor debulking | IVb | Peritoneum | – | – | – | – | NED (6 m) | Levine |
| 16 | Ovary | 18 | RSO | I | – | Abdomen, retrosternal and retroperitoneal nodes (1 m) | Ifosfamide, etoposide | PD | – | DOD (2 m) | Leath |
| 17 | Ovary | 36 | TAH, BSO | IV | Lung | – | – | – | – | DOC (2 weeks) | Stastny |
| # | Ovary | 19 | TAH, BSO, PLN, PAN | IIIc | Paraaortic lymphnode, cul-de-sac | Abdomen, paraaortic lymphnode (2 m) | Ifosfamide, epirubicin, cisplatin | CR | SD | AWD (18 m) | |

#: present case; BSO: bilateral salpingo-oophorectomy; TAH: total abdominal hysterectomy; SH: supracervical hysterectomy; PLN: pelvic lymphadenectomy; PAN: paraaortic lymphadenectomy; CR: complete response; DOD: died of disease; PR: partial response; DOC: died of complications; SD: stable disease; AWD: alive with disease; PD: progressive disease; NED: no evidence of disease; NA: not available; NE: not evaluable; ILD: inguinal lymphadenectomy.

returned to normal. She was treated with a further two courses of IEP chemotherapy. Her subsequent course was discontinued because she refused any further therapy due to severe nausea. She was clinically disease-free until 9 months following treatment, when enlarged paraaortic lymphnodes were detected by a CT scan. The patient underwent combination chemotherapy with only ifosfamide and cisplatin (she refused the inclusion of epirubicin because of anxiety for nausea). After the third course of the chemotherapy, sacral bone metastasis was found and a total 60 Gy of palliative irradiation was given. She is still alive with stable disease 18 months after the surgery.

## Discussion

MRT was first described as a distinctive, highly malignant round cell neoplasm of the kidney in children. Those tumors are aggressive, are often widely metastatic at diagnosis, thus responding poorly to therapy, and they are uniformly fatal, except for localized disease. The diagnosis is based on light microscopic findings with supportive immunohistochemistry. The term "rhabdoid" refers to a histological resemblance to rhabdomyoblasts, although muscle markers are absent. Malignant extrarenal rhabdoid tumors are subsequently recognized and they have been reported to occur at various sites throughout body, such as the central nervous system, orbit, tongue, gum margin, esophagus, stomach, liver, colon, bladder, soft tissue, and extremities. The prognosis of extrarenal disease is also extremely poor similar to renal disease.

MRT in the female genital tract is rare, with only nine cases of the vulva [3–9], six cases of the uterine corpus [10–15], and only two cases of the ovary [1] being reported so far (Table 1). The initial treatment was surgery in all cases and 10 out of 14 completely resected cases the tumor recurred rapidly i.e., within 3 months, including present case. The most frequent recurrent pattern was local recurrence in cases of vulvar MRTs. The common recurrent sites were the pelvic and paraaortic lymphnodes and the lung. In 10 patients salvage chemotherapy was given for residual or recurrent tumors. The chemotherapy regimen tends to vary in each case including adriamycin, ifosfamide, cisplatin, etoposide, and others. All patients whose response was described in the report had progressive disease except for one partial response in a vulvar MRT patient. Seven patients received radiotherapy but it did not appear to be of any benefit. Eleven out of the 17 patients reported to date died with recurrence and systemic metastases (one case died of complications after surgery), and 9 of those died within 12 months of the diagnosis.

Primary ovarian cases are extremely rare, with only two cases previously reported in 18- and 36-year-old women [1,2]. The former case was stage I and the tumor was completely resected at the surgery. Shortly after the surgery, a recurrent tumor was detected in the pelvis, cul-de-sac, omentum, and retroperitoneal lymphnode. Combination chemotherapy with ifosfamide and etoposide for recurrent tumors was initiated; however, the disease progressed rapidly, and the patient died of disease 54 days after the initial presentation. The latter case was stage IV with lung metastasis and the patient died of complications 2 weeks after surgery.

Because of the small number of cases reported in the literature, no consensus exists regarding the standardized treatment or combination of treatments to effectively deal with the disease. In general, only a surgical extirpation is considered to provide the chance for controlling MRT because chemotherapy and radiotherapy have been minimally beneficial.

The surgical management of young patients with an ovarian mass can be complex because of concern regarding the preservation of fertility. In our case, the patient and her family desired standard management of her ovarian cancer; as such, she underwent an abdominal total hysterectomy, bilateral salpingo-oophorectomy, and pelvic and paraaortic lymphadenectomy. Given the progressive nature of the tumor of the patient described in this report, extensive surgical debulking should be performed especially in patients with advanced stages.

Various combination of chemotherapeutic agents, such as adriamycin, ifosfamide, etoposide, and cisplatin, have been tried in advanced or recurrent cases of MRT in the female genital tract with little benefit in one case with a brief response by adriamycin. For renal MRT, Roper et al. reported a patient who had a complete remission induced by cisplatin and adriamycin [16]. Our present case is the first patient to demonstrate a complete clinical response after salvage chemotherapy for MRT in the female genital tract. Unfortunately she experienced recurrence, but she has been able to survive for 18 months after surgery, which is a relatively better prognosis than that of the previously reported cases. Although the best treatment has yet to be determined, the prognosis might improve if the combination chemotherapy promptly initiated after surgery.

Based on the results for this single patient, IEP chemotherapy is thus considered to be potentially useful in the treatment of MRT of the ovary. Further experience is needed to confirm that this regimen may indeed result in a better prognosis.

## References

[1] Leath III CA, Huh WK, Conner M, Barnes III MN. Primary extrarenal rhabdoid tumor of the ovary. A case report. J Reprod Med 2003;48: 283–6.

[2] Stastny JF, Harris AC, Ben-Ezra J, Nasim S, Frable WJ. Rhabdoid cells in peritoneal fluid. A case report. Acta Cytol 1996;40:1289–92.

[3] Tzilinis A, Clarke LE, Affuso C, Fessenden J. Successful treatment of malignant rhabdoid tumor of the vulva in an older patient: a case report and review of the literature. Curr Surg 2002;59:570–1.

[4] Brand A, Covert A. Malignant rhabdoid tumor of the vulva: case report and review of the literature with emphasis on clinical management and outcome. Gynecol Oncol 2001;80:99–103.

[5] Sert MB, Onsrud M, Perrone T, Abbas F, Currie JL. Malignant rhabdoid tumor of the vulva. Case report. Eur J Gynaecol Oncol 1999;20:258–61.

[6] Igarashi T, Sasano H, Konno R, Sato S, Namiki T, Ohtani H, et al. Malignant rhabdoid tumor of the vulva: case report with cytological, immunohistochemical, ultrastructural and DNA ploidy studies and a review of the literature. Pathol Int 1998;48:887–91.

[7] Lupi G, Jin R, Clemente C. Malignant rhabdoid tumor of the vulva: a case report and review of the literature. Tumori 1996;82:93–5.

[8] Matias C, Nunes JF, Vicente LF, Almeida MO. Primary malignant rhabdoid tumour of the vulva. Histopathology 1990;17:576–8.

[9] Perrone T, Swanson PE, Twiggs L, Ulbright TM, Dehner LP. Malignant rhabdoid tumor of the vulva: is distinction from epithelioid sarcoma possible? A pathologic and immunohistochemical study. Am J Surg Pathol 1989;13:848–58.

[10] Levine PH, Mittal K. Rhabdoid epithelioid leiomyosarcoma of the uterine corpus: a case report and literature review. Int J Surg Pathol 2002;10: 231–6.

[11] Gaertner EM, Farley JH, Taylor RR, Silver SA. Collision of uterine rhabdoid tumor and endometrioid adenocarcinoma: a case report and review of the literature. Int J Gynecol Pathol 1999;18:396–401.

[12] Hsueh S, Chang TC. Malignant rhabdoid tumor of the uterine corpus. Gynecol Oncol 1996;61:142–6.

[13] Niemann TH, Goetz SP, Benda JA, Cohen MB. Malignant rhabdoid tumor of the uterus: report of a case with findings in a cervical smear. Diagn Cytopathol 1994;10:54–9.

[14] Cattani MG, Viale G, Santini D, Martinelli GN. Malignant rhabdoid tumour of the uterus: an immunohistochemical and ultra-structural study. Virchows Arch A Pathol Anat Histopathol 1992; 420:459–62.

[15] Cho KR, Rosenshein NB, Epstein JI. Malignant rhabdoid tumor of the uterus. Int J Gynecol Pathol 1989;8:381–7.

[16] Roper M, Parmley RT, Crist WM, Kelly DR, Hyland CH, Salter M. Rhabdoid tumor of the kidney: complete remission induced by cis-platinum and adriamycin. Med Pediatr Oncol 1981;9:175–80.

# Identification of FAZF as a Novel BMP2-Induced Transcription Factor During Osteoblastic Differentiation

Ryuji Ikeda,[1] Kenichi Yoshida,[2]* and Ituro Inoue[3]

[1]Department of Clinical Pharmacy and pharmacology, Graduate School of Medical and Dental Sciences, Kagoshima University, 8-35-1 Sakuragaoka, Kagoshima 890-8520, Japan
[2]Department of Life Sciences, Graduate School of Agriculture, Meiji University, 1-1-1 Higashimita, Tama-ku, Kawasaki, Kanagawa 214-8571, Japan
[3]Division of Molecular Life Science, School of Medicine, Tokai University, Bohseidai, Isehara, Kanagawa, 259-1193, Japan

**Abstract** Bone morphogenetic protein 2 (BMP2) is a key factor in the regulation of osteoblastic differentiation; however, its downstream mediators are not fully understood. Previously, we identified and characterized transcription factor promyelocytic leukemia zinc finger protein (PLZF), composed of an N-terminal BTB/POZ and C-terminal zinc finger motifs, as an upstream factor of CBFA1 (Runx2/core-binding factor 1). PLZF was induced in an osteoblastic differentiation medium, but was not induced by BMP2. Here, we report the identification of transcription factor fanconi anemia zinc finger protein (FAZF), which is closely related to PLZF. FAZF was induced by BMP2 in human mesenchymal stem cells (hMSCs). In addition to the full-length FAZF, we also identified alternatively spliced mRNAs in which the C-terminal zinc finger motifs were deleted (designated BTB/POZ-only FAZF). Both the full-length and BTB/POZ-only FAZF mRNAs were equally expressed in BMP2-treated hMSCs. The full-length FAZF was exclusively detected in the nucleus, whereas the BTB/POZ-only FAZF protein was localized in the cytoplasm of the transfected cells. The full-length FAZF, but not the BTB/POZ-only FAZF, increased the expression of osteoblastic differentiation markers, including CBFA1, collagen 1A1, osteocalcin, and alkaline phosphatase in C2C12 cells. In conclusion, both FAZF and PLZF differentially participate in the regulation of osteoblastic differentiation via the BMP2 and CBFA1 signaling pathways, respectively. J. Cell. Biochem. 101: 147–154, 2007. © 2006 Wiley-Liss, Inc.

**Key words:** FAZF; BMP2; osteoblastic differentiation

Bone morphogenetic proteins (BMPs) are multi-functional growth factors that belong to the transforming growth factor β (TGFβ) super-family [see review in Chen et al., 2004]. Signal transduction studies have revealed that Smad1, 5, and 8 are downstream mediators of type I and II BMP receptors and play a critical role in BMP signal transduction. Phosphorylated Smad1, 5, and 8 proteins form a complex with Smad4 and

are then translocated into the nucleus. This signaling axis regulates the master regulators of bone cell differentiation, such as CBFA1 (Runx2/core-binding factor 1) and its downstream target osterix [Ducy et al., 1997; Nakashima et al., 2002]. Recently, we characterized the roles of promyelotic leukemia zinc finger (PLZF) in the regulation of osteoblastic differentiation of human mesenchymal stem cells (hMSCs) and C2C12 cells [Ikeda et al., 2005]. In C2C12 cells, the overexpression of PLZF increased the expression of CBFA1. On the other hand, the overexpression of CBFA1 did not affect the expression of PLZF. These findings indicate that PLZF plays important roles in early osteoblastic differentiation as an upstream regulator of CBFA1. Interestingly, PLZF nullizygous mice exhibited a limb development defect involving all proximal cartilage condensations in the hindlimb [Barna et al., 2005].

Among BMPs, preclinical and clinical studies have shown that BMP2 can be utilized in various therapeutic interventions for bone defects, non-union fractures, spinal fusion, osteoporosis, and root canal surgery as well as for craniofacial and tooth regeneration [Nakashima and Reddi, 2003]. BMP2 signaling is regulated at different molecular levels, but the molecular events downstream of BMP2 signaling that result in tissue specific gene expression and limb or skeletal development have been only partially elucidated [Johnson and Tabin, 1997]. Indeed, the expression of PLZF was unaffected by the addition of BMP2 [Ikeda et al., 2005]. Fanconi anemia zinc finger (FAZF), a member of the BTB/POZ family of transcriptional regulator proteins [Stogios et al., 2005], has the highest known degree of homology to the PLZF protein and has been shown to bind to both PLZF and Fanconi anemia complementation group C (FANCC), the protein that is defective in patients with bone marrow failure syndrome [Hoatlin et al., 1999]. FAZF is expressed at high levels in the early stages of differentiation but declines during subsequent differentiation into erythroid and myeloid lineages, and the enforced expression of FAZF is accompanied by accumulation in the $G_1$ phase of the cell cycle, followed later by apoptosis [Dai et al., 2002]. These results suggest an essential role for FAZF during the proliferative stages of primitive hematopoietic progenitors; however, its precise roles in other forms of cell differentiation remain unknown.

In the present study, we focused on characterizing the roles of FAZF in BMP2-induced osteoblastic differentiation. The upregulation of FAZF, but not of PLZF mRNA expression, was observed during BMP2-induced osteoblastic differentiation. Moreover, an alternatively spliced form of FAZF, which lacked three C-terminal C2H2 zinc finger motifs, was also induced by BMP2 treatment but did not increase the expression of osteoblastic differentiation markers. These results suggest that FAZF activity may be linked to a transcriptional regulation pathway involved in BMP2-regulated osteoblastic differentiation.

## MATERIALS AND METHODS

### Plasmid Construction

Full-length (1–487 amino acid residues) and C-terminal zinc finger motifs-deleted FAZF

(1–293 amino acid residues) cDNAs were amplified using PCR and the following primers: 5'-cggaattcgccgccatgtccctgccccccataagactgccca-gc-3', 5'-cccaagcttctgttcccgccagacctcctgccaggct-cc-3', and 5'-cccaagcttggtggtggaggaagaa-gga-caacagggaga-3'. Human Universal QUICK-Clone II (Clontech) was used as a cDNA template. The resulting PCR products were digested using EcoRI/HindIII and subcloned into a pCMV-Tag 4A vector (Stratagene), which contains a C-terminal Flag tag; sequencing analyses were then performed.

### Cell Culture and Transfections

hMSCs, purchased from BioWhittaker (Walkersville, MD), and mouse pluripotent mesenchymal precursor cells (C2C12) were cultured in Dulbecco's modified Eagle's medium (DMEM) containing 10% fetal bovine serum (FBS) and an antibiotic/antimycotic solution (100 U/ml penicillin, 100 µg/ml streptomycin, and 250 ng/ml amphotericin B) (Sigma). The osteogenic differentiation (OS) medium has been previously described [Ikeda et al., 2005]. Human recombinant BMP2 was purchased from Sigma. The C2C12 cells were transfected with pCMV-Tag 4A expression vector containing FAZF with lipofectamine 2000. After 48 h, the cells were harvested and subjected to RT-PCR or immunohistochemistry analyses.

### RT-PCR

Total cellular RNA was extracted using a Trizol reagent according to the manufacturer's instructions. RT-PCR was performed using a SuperScript One-Step RT-PCR system (Invitrogen) with gene specific primers, according to the manufacturer's instruction. Reactions containing the total RNA (500 ng of each), 0.2 mM of dNTPs, 0.2 µM of each primer, an enzyme mixture composed of SuperScript II reverse transcriptase and Platinum $Taq$ DNA polymerase, and a reaction buffer composed of 1.2 mM $MgSO_4$ were incubated at 50°C for 30 min and than at by 94°C for 2 min; PCR was then performed as follows: 30 cycles of 94°C for 15 sec, 55°C for 30 sec, and 70°C for 1 min. The primer sets for the RT-PCR reactions were designed based on human and mouse sequences in GenBank as follows: human FAZF, 5'-acaggc-gcacttgcaacctgtg-3' and 5'-gcatgtgcgcctgcatg-gaggc-3'; human FAZF (forward primer in exon 2 and reverse primer in exon 5),

5'-cagcctgccctgtggagcatcctgctgatg-3' and 5'- gca-cgcatagggccgagaccgagcaggagg-3'; human PLZF, 5'-tctcaaacgccacctgcgctcacat-3' and 5'-cactgg-cagggcgaggcgccgttgt-3'; mouse CBFA1, 5'-acctc-tgacttctgcctctggc-3' and 5'-atgctgacga-agtacca-tagta-3'; mouse ALP, 5'-accttgactgtggttactgctg-3' and 5'-gacgccgtgaagcaggtgtgcc-3'; mouse collagen1A1, 5'-cctggtgaatctggacgtgagg-3' and 5'-gaccagagaagccacgatgacc-3'; mouse osteocal-cin, 5'-aggtagtgaacagactccggcg-3' and 5'-ctggtc-tgatagctcgtcacaa-3'; human GAPDH, 5'-agaa-catcatccctgcctctactgg-3' and 5'-aaaggtggaggagt-gggtgtcgctg-3'; and mouse GAPDH, 5'-ccgcctgga-gaaacctgccaag-3' and 5'-ggataggggcct-ctcttgctc-ag-3'. 

### Measurement of Alkaline Phosphatase (ALP) Activity

ALP activity was histochemically measured using staining kit No. 85L-3R (Sigma). Briefly, cells were fixed with citrate-buffered acetone for 30 sec followed by washing with deionized water for 45 sec; the cells were then incubated with an alkaline-dye mixture for 30 min at room temperature in the dark.

### Immunofluorescent Staining

Cells cultured on cover slips were washed twice with phosphate-buffered saline (PBS) and fixed with 2% paraformaldehyde for 20 min at room temperature. After washing three times with PBS, the cells were permeabilized with 0.3% Triton-X100 for 10 min at room tempera-ture. After blocking with 3% skim milk in PBS for 30 min, the cells were incubated for 1 h with anti-Flag monoclonal antibody diluted 1:100 in PBS containing 3% skim milk. After washing three times with PBS, the cells were incubated for 20 min with Cy5- or Cy3-conjugated anti-mouse sheep IgG diluted 1:100 in PBS contain-ing 3% skim milk. The cells were then washed three times with PBS, and the immunolocaliza-tions patterns were examined using fluores-cence microscopy (Olympus).

## RESULTS

### Identification of FAZF as a BMP2-Induced, but not an Osteogenic Differentiation (OS) Medium-Induced, Transcription Factor During Osteoblastic Differentiation

Previously, we identified PLZF as an OS medium (0.1 μM dexamethasone, 0.05 mM ascorbic acid-2-phosphate, and 10 mM β-glycer-ophosphate)-induced transcription factor that was active during osteoblastic differentiation [Ikeda et al., 2005]. We then asked whether FAZF, the most closely related known protein to PLZF [Lin et al., 1999], could be induced during osteoblastic differentiation. To answer this question, we first treated hMSCs with OS medium, since hMSCs differentiate into osteo-genic cells in the presence of OS medium [Pittenger et al., 1999]. Treatment of the hMSCs with OS medium for 6 days greatly increased ALP activity (Fig. 1A). Total RNA extracted from the hMSCs on days 0 and 2 of the OS treatment was then subjected to RT-PCR analysis. Consequently, we observed that the mRNA expression of PLZF, but not of FAZF, was upregulated during the early stage of osteogenic differentiation (Fig. 1B).

Next, we tested whether BMP2 could induce FAZF mRNA expression in hMSCs. BMP2 is known to play important roles in bone formation and osteoblastic differentiation [Yamaguchi et al., 1991; Katagiri et al., 1994] and, more specifically, to induce CBFA1 expression [Lee et al., 2000]. Several studies have shown that BMP2 induces hMSCs to differentiate into osteoblastic cells [Katagiri et al., 1994; Lee et al., 2000]. In our assay, ALP activities were enhanced by BMP2 treatment in a
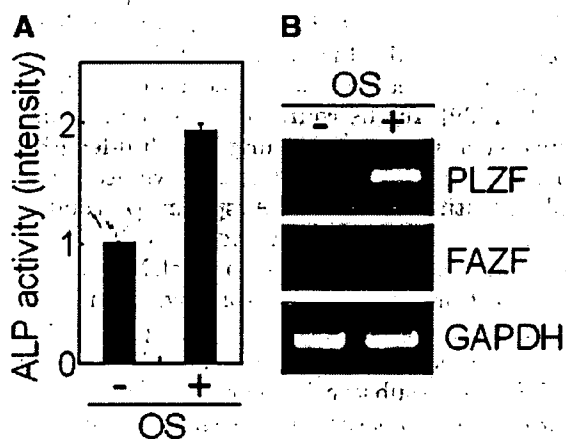


**Fig. 1.** Expression of PLZF and FAZF during the OS medium-induced osteoblastic differentiation of hMSCs. A: ALP activity in hMSCs. Cells were cultured in medium with or without OS for 6 days. ALP staining was performed as described in the Materials and Methods section, and the intensity was determined using an NIH imager. Experiments were performed at least three times; the mean and SD are shown. B: Expression of PLZF and FAZF in hMSCs after OS treatment. Cells were cultured for 48 h in the presence or absence of OS. Total RNA was extracted, and RT-PCR was performed using GAPDH as a standard.
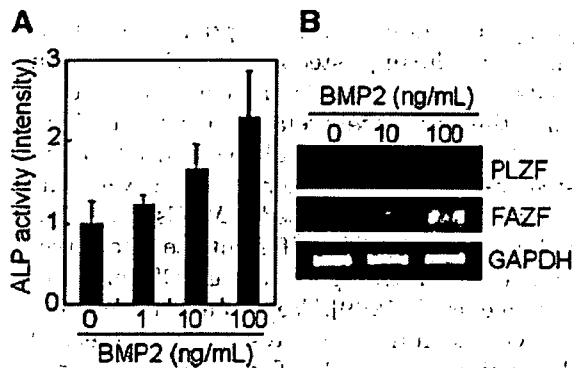
**A**                    **B**



Fig. 2. Expression of PLZF and FAZF during BMP2-induced osteoblastic differentiation of hMSCs. A: hMSCs were cultured in the presence or absence of BMP2 (0–100 ng/ml). Six days later, ALP activity was determined by ALP staining, as described in Figure 1A. B: hMSCs were cultured in the presence or absence of BMP2 (10 or 100 ng/ml). Total RNA was extracted after 72 h of treatment, and the expression of PLZF, FAZF, and GAPDH mRNA was examined using RT-PCR.

dose-dependent manner (Fig. 2A). Surprisingly, BMP2 enhanced the expression of FAZF, but not of PLZF (Fig. 2B). These results suggest that PLZF and FAZF are differentially involved in the regulation of osteoblastic differentiation.

### Full-Length FAZF, but not Zinc Finger Motifs-Deleted (BTB/POZ Domain-Only) FAZF, Increased the Expression of Osteoblastic Differentiation Markers

The predicted full-length FAZF cDNA (RefSeq no. NM_014383) is 1,960 base pairs long and encodes a 487-amino acid protein [Lin et al., 1999]. In the course of constructing an expression vector containing the full-length open reading frame FAZF cDNA, we accidentally identified two mRNA splicing variants (hereafter called variant 1 and 2). Sequencing analyses revealed that the novel cDNAs were derived from alternative splicing, resulting in out-of-frame transcripts (see Fig. 3A and discussion below). As illustrated in Figure 3B, FAZF shows a substantial degree of homology to PLZF throughout the entire region, except for the number of zinc finger motifs located in the C-terminus [Lin et al., 1999]. The full-length FAZF consisted of six exons, and exons 2–6 were translated into wild-type FAZF protein (Fig. 3C). FAZF has two characteristic domains, a BTB/POZ domain encoded by exon 2 and a region containing three zinc finger motifs encoded by exon 6. The BTB/POZ domain acts as a specific protein-protein interaction domain

[Stogios et al., 2005]. On the other hand, the C-terminal PLZF-like C2H2 zinc fingers are known to bind to the TGTACAGTGT motif located at the upstream flanking sequence of the Aie1 gene [Tang et al., 2001]. An earlier report identified an alternatively spliced isoform that lacked exon 4 but transcribed the in-frame regions between exon 1+2+3 and exon 5+6, resulting in a 474-amino-acid that was virtually the same as the wild-type FAZF protein [Lin et al., 1999]. We called this protein wild-type 2, and the full-length FAZF protein will hereafter be referred to as wild-type 1 (Fig. 3C). On the other hand, exon 3 of variant 1 and exons 3+4 of variant 2 are alternatively spliced-out (not transcribed into mRNAs), resulting in the appearance of stop codons in exons 4 and 5, respectively. The resulting proteins are 311- and 302-amino acids for variants 1 and 2, respectively. These variants lack the C-terminal zinc finger motifs but have a distinct C-terminal tail (Fig. 3A).

To substantiate the expression patterns of full-length and BTB/POZ-only FAZF during osteoblastic differentiation, we performed an RT-PCR analysis using mRNA from hMSCs treated with BMP2 (100 ng/ml). For this purpose, primers for exons 2 and 5 were designed (see Fig. 3C). This enabled us to distinguish mRNA species; namely, PCR amplification resulted in a 351-bp product for the full-length mRNA (wild-type 1, exon 2+3+4+5), a 282-bp product for the wild-type 2 mRNA (exon 2+3+5), a 277-bp product for variant 1 (exon 2+4+5), and a 208-bp product for variant 2 (exon 2+5). After three days of incubation with BMP2, two major bands smaller than 350-bp were equally amplified (Fig. 3D). Sequencing analyses showed that the faster and slower migrating bands corresponded to variant 2 (208-bp) and wild-type 2 (282-bp)/variant 1 (277-bp), respectively. These results suggested that BMP2 induced both wild-type FAZF and BTB/POZ-only FAZF during the BMP2-induced osteoblastic differentiation of hMSCs.

To determine the cellular localization of full-length and BTB/POZ-only FAZF, we transfected C2C12 cells with a control vector or an expression vector encoding full-length or BTB/POZ-only FAZF cDNA. After 48 h, the cells were fixed and visualized using fluorescence microscopy. Full-length FAZF was exclusively detected in the nucleus, whereas BTB/POZ-only FAZF protein was localized in the cytoplasm of